# COUPLING TRANSITIONS FOR TRAVELING WAVE TUBES

WILLIAM J. HENNINGSEN

Library
U. S. Naval Postgraduate School
Monterey, California

# COUPLING TRANSITIONS
# FOR
# TRAVELING WAVE TUBES

* * *

William J. Henningsen

# COUPLING TRANSITIONS
# FOR
# TRAVELING WAVE TUBES

by

William J. Henningsen

Lieutenant, United States Navy

Submitted in partial fulfillment

of the requirements

for the degree of

MASTER OF SCIENCE
IN
ENGINEERING ELECTRONICS

United States Naval Postgraduate School
Monterey, California

1955

Thesis
H45

Library
U. S. Naval Postgraduate School
Monterey, California

This work is accepted as fulfilling
the thesis requirements for the degree of

MASTER OF SCIENCE

IN

ENGINEERING ELECTRONICS

from the

United States Naval Postgraduate School

# PREFACE

The traveling wave tube with its ability to amplify over tremendous bandwidths promises to become the keystone of future developments in microwave equipment for transmission of information and in military countermeasures work. The drawback of insufficient bandwidth in conventional microwave tubes has been replaced by the problem of developing efficient methods of utilizing the bandwidth available in the traveling wave tube. However, there are still many difficulties involved in the design and manufacture of efficient traveling wave tubes. Not the least of these is the problem of coupling radio frequency energy into and out of the tube. The object of this paper is to discuss some of the aspects of this coupling problem and how it applied to a particular tube.

The writer wishes to express his appreciation to Dr. W. M. Bauer for his encouragement and criticism. The work included here was done under the supervision of Dr. C. W. Barnes and Mr. R. E. Vehn of the Sylvania Microwave Tube Laboratory, whose assistance and cooperation is gratefully acknowledged.

# TABLE OF CONTENTS

| Item | Title | Page |
|---|---|---|
| CHAPTER I | Introduction . . . . . . . . . . . . . . . . . | 1 |
| CHAPTER II | Impedance of a Helix in Free Space . . . . . . . . . . . . . . . . . | 4 |
| CHAPTER III | Effects of Surroundings on the Helix Impedance . . . . . . . . . . | 17 |
| CHAPTER IV | Methods of Coupling Between Transmission Line and Helix . . . . . . . . . . . . . | 24 |
| CHAPTER V | Design of Particular Coupling Systems . . . . . . . . . . . . . | 35 |
| BIBLIOGRAPHY | . . . . . . . . . . . . . . . . . . . . . . . | 42 |

# LIST OF ILLUSTRATIONS

| Figure | | Page |
|---|---|---|
| 1. | Sheath Helix Model . . . . . . . . . . . . . . . . | 43 |
| 2. | Dispersion Curve of the Sheath Helix . . . . . . | 43 |
| 3. | Equivalent Circuit for Helix Assuming Distributed Constants . . . . . . . . . . . . . . | 44 |
| 4. | Developed Sheath Helix Model . . . . . . . . . . | 44 |
| 5. | Effect of Wire Size on Interaction Impedance. . . | 44 |
| 6. | Effect of Wire Size on Transverse Impedance . . . | 45 |
| 7. | Ratio of Interaction Impedance at Longest Allowable Radius to Interaction Impedance at Surface of Developed Sheet . . . . . . . . . . | 45 |
| 8. | Tape Helix Model . . . . . . . . . . . . . . . . | 46 |
| 9. | Propagation Constants of Tape Helix Model . . . . | 46 |
| 10. | Equivalent Circuit of Tape Helix Model . . . . . | 46 |
| 11. | Mode Impedances of Tape Helix Model . . . . . . . | 47 |
| 12. | Effect of Dielectric on Sheath Helix . . . . . . | 48 |
| 13. | Sheath Helix With External Shield . . . . . . . . | 48 |
| 14. | Dispersion Characteristics of Sheath Helix With External Shield . . . . . . . . . . . . . . | 49 |
| 15. | Power-Current Impedance Factor for Sheath Helix With External Shield . . . . . . . . . . . | 50 |
| 16. | Rectangular Waveguide Coupling System . . . . . . | 51 |
| 17. | Cavity Coupling System . . . . . . . . . . . . . | 51 |
| 18. | Tapered Helix With External Shield . . . . . . . | 52 |
| 19. | Helix With Tapered Pitch . . . . . . . . . . . . | 52 |
| 20. | Equivalent Circuit and Configuration for Stub Compensated Transition . . . . . . . . . . . . | 53 |
| 21. | Configuration for Stub Compensated Transition Using Strip Line Technique . . . . . . . . . . | 53 |
| 22. | Coupled Helix Transition . . . . . . . . . . . . | 54 |

23. Voltage Variation Along Coupled Helices . . . . . . . . . 54

24. Coefficient of Coupling as a Function of Helix Radii and Frequency . . . . . . . . . . . . . . . 55

25. Variation of $q\beta\ell$ and coupling Loss With Frequency and Helix Radii . . . . . . . . . . . . . 56

26. Tapered Shield Transition . . . . . . . . . . . . . . . 56

27. Plot of VSWR vs. Frequency for Tapered Shield Transition 57

28. Plot of Transmitted Power vs. Frequency for Tapered Shield Transition . . . . . . . . . . . . . . . 58

29. Tapered Shield Transition For Ruggedized Tube . . . . . . 59

30. Plot of VSWR vs. Frequency for Tapered Shield in Ruggedized Tube . . . . . . . . . . . . . . . . . . 60

31. Plot of Transmitted Power vs. Frequency for Tapered Shield in Ruggedized Tube . . . . . . . . . . . 61

32. Plot of VSWR vs. Frequency for Coupled Helix Transition . 62

33. Plot of Transmitted Power vs. Frequency for Coupled Helix Transition . . . . . . . . . . . . . . . . . . 63

# TABLE OF SYMBOLS AND ABBREVIATIONS

$B$ - Distributed Shunt Admittance
$C$ - A Gain Parameter Defined by Pierce, Ref. 8
$E$ - a c Electric Field
$F$ - Impedance Reduction Factor Defined by Tien, Ref. 12
$F(\ a)$ - A factor in the Formula for Interaction Impedance
$I$ - Complex a c Current
$I^*$ - Conjugate of Complex a c Current
$I_0$ - d c Beam Current
$I_0(\ a)$ - Modified Bessel Function of the First Kind
$K_e$ - Longitudinal Helix Impedance
$K_t$ - Transverse Helix Impedance
$L$ - Turn Length of Helix
$P$ - Power
TPI - Turns Per Inch
$V$ - Complex a c voltage
$X$ - Distributed Series Reactance
$Z$ - Complex Impedance
$a,b$ - Mean Radii of Helices
$b,c$ - Radius of External Shield
$c$ - Velocity of Electromagnetic Waves in Free Space
$d$ - Diameter of Helix Wire
$k$ - Phase Constant of Electromagnetic Waves in Free Space
$p$ - Pitch of Helix

$q$ - Coupling Coefficient

$v$ - Phase Velocity of Axial Wave

$\beta$ - Axial Phase Constant

$\gamma$ - Radial Phase Constant

$\Gamma$ - Propagation Constant

$\psi$ - Pitch Angle of Helix

$\omega$ - Angular Frequency in Radiams per Second

$\delta$ - Width of Wire in Tape Helix Model

# CHAPTER I

# INTRODUCTION

Since the discovery of the broadband capabilities of the traveling wave type of microwave tube, one of the major problems has been that of the transition from conventional transmission lines to the helical slow wave structure that is normally used. Traveling wave tube amplifiers and backward wave oscillators with bandwidths of two to one and greater are commonplace, but the methods of coupling radio frequency energy into and out of them to take full advantage of this bandwidth still pose difficulties in design and construction to the tube engineer.

The distinguishing feature of a traveling wave tube is a slow wave structure for the propagation of radio frequency energy. This may take many forms but the inherent broadband capabilities of a helix and its simplicity of construction make it a natural choice. In addition, the helix has a high axial component of electrical field which is a fundamental requirement for amplification to take place. Conventionally, radio frequency energy is conveyed either by waveguide or coaxial cable which have impedances quite different from a helix. Hence, in order to match the different impedances, a transition between the two propagating structures is always required at both the input and output of a traveling wave tube. Among the desirable characteristics of such a transition are the following:

A. The transition should add no axial length to the tube and the diameter should be no greater than the gun structure.

B. The transition should have a bandwidth equal to or greater than

the operating bandwidth of the tube. This is usually defined as a SWR of 1.5 to 1 over the required bandwidth.

C. The transition should not radiate and should be shielded from external radiation.

D. The transition should have a low insertion loss.

E. The helix should have external connections suitable for monitoring currents or for handling heating currents during processing. In practice, these requirements are seldom completely achieved.

In order to transform from one impedance to another, it is important to know each of the impedances between which the transformation is desired. The characteristic impedance of coaxial cable is easily computed and the wave impedance of a waveguide may be defined. However the circuit impedance of a helix is a somewhat indefinite quantity. The impedance of a long helix is related to the interaction between the propagated waves and the electron beam, but at the ends of the helix where the matching section must be placed, this impedance is altered in an indeterminate manner by the mechanical structures near the helix, the end effects of the helix, and the unavoidable discontinuities in the matching section. A good match is important for another reason. In all amplifiers loss must be added to the helix so that the backward loss is greater than the forward gain. This will prevent oscillations due to reflections at the input and output ends. The backward loss can be reduced and hence the forward gain increased if a good broadband match at the couplers can be obtained.

This thesis will discuss the various impedance parameters that

have been developed by different investigators and the relation of these parameters to the matching problem. Various methods of coupling to the helix will be summarized and the particular methods used by the author for experimental couplers to an X band tube will be discussed in detail.

# CHAPTER II

# IMPEDANCE OF A HELIX IN FREE SPACE

## 1. Sheath helix model.

No exact analysis of the propagation along a physical helix has ever been accomplished. However, a useful and relatively simple approach to the analysis of a helical transmission line is the sheath helix. The analysis introduced by J. R. Pierce in 1947 is probably the most realistic and useful. /8, 9/. The sheath helix model used in this analysis is as shown in Fig. 1. It takes the form of a cylindrical sheet of infinitesimal thickness which conducts only in the helical direction at an angle $\psi$ . In this analysis only those modes of propagation with no angular variations are considered. This may be called the zero order mode. This limitation of the analysis to modes with no angular dependency is justified on the basis that the fields about the helix as used in a traveling wave tube do not vary appreciably with the angular coordinate. In a traveling wave tube amplifier, interaction is desired between the electron stream and the axial electrical field. To achieve a strong axial electric field, the helix parameters are chosen so that a wave length along the helix usually covers several turns.

The field solution for the sheath helix follows from a solution of the wave equation in cylindrical coordinates with cylindrical symmetry. The boundry conditions imposed at the cylindrical surface are as follows: the electric field along the helical direction is zero; the electrical field normal to the helical direction is continuous through the sheath; the magnetic field tangent to the helical direction is continuous through

the sheath. The resulting solution to the wave equation, subject to these boundary conditions, is a wave with axial dependency of the form $e^{-jbz}$, and radial dependency in the form of a modified Bessel function with argument $\gamma a$, where $\gamma^2 = \beta^2 - k^2$, $\beta = \omega/v$, $k = \omega/c$, $v$ = phase velocity of axial wave, $c$ = velocity of light, and $\omega$ = angular velocity in radians per second. The solution for the propagation constant assumes a determinantal form;

$$(\gamma a)^2 \qquad \frac{I_0(\gamma a)\, K_0\, (\gamma a)}{I_1(\gamma a)\, K_1\, (\gamma a)} = (k\, a \cot \psi)$$

The significance of this transcendental expression is best shown by a plot with normalized coordinates as in Fig. 2. Qualitatively, the ordinate is proportional to the phase velocity and the abscissa is proportional to frequency. It is apparent that for large values of $k\, a \cot \psi$, i.e. high frequency for a given helix, the value of $k/\gamma \cot \psi$, which is proportional to phase velocity, approaches one and $\gamma$ becomes approximately equal to $k \cot \psi$. For small values of $k \cot \psi$ the helix is dispersive, i.e., the phase velocity decreases as the frequency increases. Therefore, for amplification the velocity of the electron stream must decrease as the frequency increases. A tube may be designed to operate in this range resulting in what is called a dispersive amplifier. It is a relatively narrow band amplifier which may be tuned electronically by varying the beam voltage. A normal broadband amplifier operates in the flat non-dispersive region where phase velocity is nearly independent of frequency. Here the phase velocity approaches the asymptatic value of $v = c \sin \psi$. Essentially, we have a TEM wave which propagates along the helix at approximately the speed of light.

## 2. Impedance relationships.

The approach used by Pierce to define the characteristic impedance of the helix is an analysis based upon the power flow along the helix and the fields about the helix. The fundamental problem in this sort of an analysis is that the helix does not propagate a pure TEM wave. Therefore, some ambiguity is involved in the selection of what might be called the characteristic components of the field which will give a representative characteristic impedance. It may be defined on a voltage-current basis, a voltage-power basis, or a current-power basis; the voltage normally being defined as the line integral of the transverse electric field between two conductors, and the current as the high frequency surface current flowing in one of the conductors. Pierce defines two helix impedances on a voltage-power basis; a transverse and a longitudinal impedance. Neither of these impedances gives full information for matching a helix to a waveguide or coaxial cable. However, in any impedance matching problem an approximate characteristic impedance is of considerable value.

The transverse impedance $K_t$ is found by integrating the radial electric field from the radius a of the helically conducting sheet to infinity, giving the transverse voltage $V_t$. The total power flowing in the axial direction is found from the field components by integrating the Poynting vector from the axis to infinity. $K_t$ is then found from the relation

$$P = \frac{V_t^2}{2K_t}$$

The resulting formula for $K_t$ is a complex expression in terms of modified Bessel functions, but which, for large values of $\gamma a$, reduces to

$$K_t = (\beta/k)\,(\gamma/\beta)^2\,(30/\gamma a)$$

The longitudinal voltage is taken as one half the integral of the longitudinal component of the electric field at the surface of the helix for one half wavelength. This integral turns out to be $(\gamma/\beta)\ V_t$. Accordingly, the longitudinal impedance $K_\ell$ is given by

$$K_\ell = (\gamma/\beta)^2\ K_t$$

Another important parameter of the helix defined by Pierce is the interaction impedance, $E_z^2\ /\ (\beta^2 P)$, which has the dimension of ohms. It is based on an equivalent circuit assuming distributed constants for the helix. The helix is considered a lossless transmission line composed of distributed series reactance $X_1$ and distributed shunt susceptance $B_c$ , and with current I and voltage V as shown in Fig. 3. A bunched electron stream with convection current i flows very close to the circuit.

These circuit constants define a characteristic impedance $K = \sqrt{X/B}$ and a propagation constant $\Gamma = j\sqrt{XB}$ in the absence of the electron stream. Since the voltages and currents vary with distance as $e^{-\Gamma z}$, differentiation with respect to z may be replaced by multiplication $-\Gamma$. Then $E_z = \partial V/\partial z = -\Gamma V$ or $V = E/\Gamma$ . Since this is a lossless circuit, $\Gamma$ can be replaced by $\beta$, which can also be taken equal to the electron phase constant since the electron velocity is, in practice, very close to the natural phase velocity of the circuit. The total power flow in the axial direction is again $P = \frac{1}{2}\ V^2/K$. From this

$$2K = V^2/P = E_z^2/(\beta^2 P)$$

As before, the power is found from the field components by integrating the Poynting vector from the axis to infinite. For the field on the axis, i.e., $E_z(0)$, the interaction impedance is thus given by

$$E_z^2(0)/(\beta^2 P) = (\beta/k)\ (\gamma/\beta)\ \ F(\gamma a)$$

where $F(\gamma a)$ is a complicated expression containing modified Bessel functions, but it is accurately given over a large range by the empirical relation

$$F(\gamma a) = 7.154\, e^{-.6664 \gamma a}$$

As usual, $\gamma/\beta$ is nearly unity for phase velocities small compared with the velocity of light and $\beta/k = c/v$. The interaction impedance relates the power flow in the circuit to the electron stream. It is a measure of the effectiveness of the circuit in producing a bunched beam. As was shown by C. C. Cutler, it can be determined experimentally by probing the fields even when it cannot be calculated analytically [1] . For a given helix $E^2/(\beta^2 P)$ is approximately proportional to $F(\gamma a)^3$ which decreases as frequency increases. Physically this is because at high frequencies, the longitudinal electric field decreases rapidly with increasing distance from the helix.

The field equations show that $E_z$ at distance r from the axis is $I_o(\gamma r)$ times the field on the axis. If $E_z$ is taken at $r = a$, the interaction impedance becomes identical with twice the longitudinal impedance $K_1$ previously mentioned. The actual electron stream is never confined to the axis; hence to find the effective value of $E^2/(\beta^2 P)$, the average value of the electric field over the beam must be used. The average value of $E_z^2$ is greater then $E_z(0)$ by a factor $\left[ I_o(\gamma r)^2 - I_1(\gamma r) \right]$ . Pierce has plotted the variation of this factor vs. $(\gamma a)$ for various ratios of beam radius to helix radius.

The interaction impedance is important because it is one of the factors in the well known gain formula

$$G = A + BCN$$

where $$C = \left[ \frac{E_z^2}{\beta^2 P} \frac{I_o}{4V_o} \right]^{1/3}$$

and $I_o$ and $V_o$ are the beam current and beam voltage respectively. C also appears in the formula for the change in the characteristic impedance of the three forward traveling waves due to the electron beam.

$$K_n = K_t(1-jC\rho_n)$$

where $\rho = (-j)^{1/3}$ is a factor used in determining the propagation constants for the three traveling waves and n = 1, 2, 3 corresponding to the three roots of $\rho$. $\rho_1$, the propagation factor for the increasing forward wave which we are interested in, is $\sqrt{3}/2-j/2$. Therefore

$$K_1 = K_t \left[1-C/2- j(\sqrt{3}/2)C\right]$$

Hence, for maximum coupling of energy to this increasing wave, a perfect matching section would account for this change in impedance. However, the sheath helix model is only approximate and C is very small so $K_t$ can be used as a starting point. Thus, to determine an impedance for matching purposes, $\gamma$ can be found from Fig. 1, $\beta$ is given by $\sqrt{\gamma^2+k^2}$, and $K_t$ can be computed from the approximate expression given previously or it can be taken from the exact curve given in Pierce.

3. The developed sheath helix.

The sheath helix obviously neglects the finite wire diameter and periodic structure of an actual helix. The periodic nature of a helix causes higher order modes and spatial harmonics which are important for a more complete analysis of traveling wave tubes, especially the backward wave oscillator. This periodicity cannot be shown with a sheath helix but Pierce investigated the effect of finite wire size by using a modification of the sheath helix which is termed a developed wire helix. For

large values of $\gamma a$, which is the usual case, the fields fall off very rapidly away from the conducting sheet. Under these circumstances a fairly accurate representation of a sheath helix may be made by slitting the conducting sheet along a spiral line normal to the direction of conduction and flattening it out as shown in Fig. 4. The fields must match at $y = 0$, $z = 2\pi a \sin\psi$ and $y = 2\pi a \cos\psi$, $z = 0$ in order that they will match when the sheet is rolled up.

The solution to the wave equation in rectangular coordinates is a plane wave traveling in the y direction with velocity c. The evaluation of $\beta$, the propagation constant in the axial direction gives $\beta = \sqrt{k^2 + \gamma^2}$ which is the same realtion obtained for a sheath helix. Here $\gamma$ is the propagation constant in the x direction. $E^2/(\beta^2 P)$ is again found by computing the power in the axial direction and the axial electric field is given by $E = E_0 \cos\psi$. From this

$$E^2/(\beta^2 P) = (\gamma/\beta)^4 (\beta/k) (60/\gamma a)$$

The longitudinal impedance is half this, and the tranverse impedance is $(\gamma/\beta)^2$ times the longitudinal impedance.

The effect of wire size may be determined by a similar developement of a wire helix, i.e., by slitting the helix along a spiral line normal to the wires. The waves propagated on the developed helix are TEM waves propagated in the direction of the wires, and the electric field normal to the direction of propagation may be found from a solution of La Place's eouation. Pierce considers two special cases, one in which the wires of the developed helix are one half wavelength long and the other in which the wires are one quarter wavelength long. Expressions are developed

which show the ratio of $E^2/\beta^2P$ and $K_t$ for each case of the developed wire helix to the developed sheath helix. The variable parameter in the expressions is the ratio of the wire diameter d to the pitch p . For example, when $d/p = .5$ the open space between wires is equal to the wire diameter. In Fig. 5 the ordinate is the factor by which $(E^2/\beta^2P)^{1/3}$ on the axis, as computed from the developed sheath helix, should be multiplied to account for the wire size. Fig. 6 shows the effect of wire size on the transverse impedance. Fig. 5 indicates that for large wire diameter $E^2/\beta^2P$ on the axis may be larger than for a helical sheet. This is because the thick wires extend nearer to the axis than the sheet. However, the effective value of $E^2/\beta^2P$ for an actual helix will be less than a helical sheet because the largest radius the beam may have is the mean helix radius a minus the wire radius. In Fig. 7, the ratio of $(E^2/\beta^2P)^{1/3}$ for this largest allowable radius to $(E^2/\beta^2P)^{1/3}$ at the surface of the developed sheet is plotted vs. d/p. This shows that there is an optimum ratio of wire diameter to pitch which is about 0.2 for both cases. However, for mechanical reasons it is best to use large wire and since the maxima are broad, most tubes are built with d/p about 0.5.

We may now make a more accurate estimate of the helix impedance than that based on the sheath helix. The dimensions of the helix are determined by optimizing the interaction impedance taking into account all the specifications of the tube. This fixes the input impedance of the helix. An exact definition of the input impedance is impossible but the transverse impedance, $K_t$, based on transverse fields and power flow is similar to the characteristic impedance of transmission lines and valuable information for matching purposes.

## 4. Tape helix model

An important improvement over the sheath helix analysis was made by S. Sensiper in his analysis of a tape helix model [10, 11]. The tape helix model as used by Sensiper and shown in Fig. 8 is a closer approach to a physical helix than the sheath helix. It is of infinitesimal thickness, has width $\delta$, radius $a$, and pitch $p$. The following boundary conditions are applied at $r = a$; the tangential electric field on the tape is zero, the magnetic field is continuous through the gap, the magnetic field discontinuity is proportional to the total current density on the tape.

Since the helix is periodic, the fields are multiplied only by some complex constant if one moves down the helix a distance $p$. A form of $z$ dependence which satisfies this requirement is

$$e^{-j\beta z} \; e^{-jm(2\pi/p)z} = e^{-j\beta_m z}$$

where
$$\beta_m = \beta + m2\pi/p$$

and $m$ can have any plus or minus integer value. Angular dependency of the solution is given by $e^{jn\theta}$. But due to the periodicity, it is evident that if the helix is translated along its axis some distance less than p, it may be rotated so that it again coincides with itself. As a result n will be equal to m. The solution to the wave equation leads to a Hertzian electric potential

$$e^{-j\beta z} \sum_m A_m \begin{matrix} I_m(\gamma_m r) \\ K_m(\gamma_m r) \end{matrix} \; e^{-jm\left[(2\pi/p)z - \theta\right]} \quad \begin{matrix} r \leqq a \\ r \geqq a \end{matrix}$$

where $I_m$ and $K_m$ are modified Bessel functions of order m and

$$\gamma_m = \sqrt{\beta_m^2 - k^2}\; a$$

The surface current density, being directly related to the magnetic field at $r = a$, must therefore have the same z and 0 dependency as the magnetic field. In addition the current must be limited to the width of the tape and be zero elsewhere. Under these restrictions the coefficient $A_m$ is expressed in a Fourier expansion across the tape.

The determinantal eouation for the propagation constant is very complex and can only be evaluated after several approximations which are based on the assumption that the tape is narrow. Fig. 9 shows the graphical solution for the particular case $\psi = 10$ degrees and $\delta/p = 0.1$. It is evident that, contrary to the sheath helix solution where $\beta$ varied continuously with k, this solution prohibits propogation in certain so called forbidden regions. The boundaries of these forbidden regions are determined by the condition that $\gamma_m$ must be real and positive, i.e., $|\beta_m| > k$. The necessity of this can be explained as follows: If a solution were possible in say the $n^{th}$ forbidden region, then all the harmonics in the external field would have radial dependence of the form $K_m(\gamma_m r/a)$ except one which would be $K_n(j\gamma_n r/a)$. A modified Bessel function with an imaginary argument becomes a Hankel function of the second kind which corresponds to an outward traveling wave. This would represent an average radial power flow which is contrary to the condition that the average power flow must be the same through any infinite plane perpendicular to the z axis if $\beta$ is real. Sensiper then presents a proof that $\beta$ must be real in a lossless system such as this.

The condition that $|\beta_m| > k$ can be written

$$|\beta a + |m| \cot \psi| > ka$$

If $\beta$ is assumed positive the above inequality is true for $m = 0$, if $|\beta| > k$. However if $m < 0$, $\beta$ is further constrained by the expression

$$|m| \cot \psi + ka < \beta a < |m| \cot \psi - ka$$

A similar expression results for negative values of $\beta$. Finally, for both positive and negative values of $\beta$ and m, $\beta$ must obey the following inecualities $$|m| + \frac{ka}{\cot \psi} < \frac{|\beta| a}{\cot \psi} < |m| - \frac{ka}{\cot \psi}$$

and $$|\beta| > k$$

These expressions thus determine the boundaries of the forbidden regions.

The branches lettered $\beta_0$, $\beta_1$, etc., refer to the dominant harmonic in that mode. In this plot the phase velocity of a wave is given by the slope of a straight line drawn to the point of interest on the curve and the group velocity by the slope of the curve at that point, i.e.,

$$\frac{v_{pm}}{c} = \frac{ka/\cot \psi}{m + \beta a/\cot \psi}$$

$$\frac{v_g}{c} = \frac{d(ka)}{d(\beta a)}$$

Hence, all the harmonics of a given mode have the same group velocity. The solid and dotted lines denote waves which would be observed if one were at $z > 0$ and $z < 0$ respectively with the source at $z = 0$. Thus, at low frequencies for $z > 0$, modes with propagation constants $-\beta_1''$, $\beta_0$, and $\beta_1'$ would be detected. Each one of these modes must contain a double infinite set of space harmonics in order to match the boundary conditions. The propagation constant of the $m^{th}$ space harmonic is

found by shifting the orgin along the $\beta a/\cot\psi$ abscissa m units. For example, the 0, 1, 2, etc. space harmonic components of the $\beta_o$ mode have positive phase velocities while the -1, -2, etc. space harmonics have negative phase velocities. Since the phase and group velocities of the -1 space harmonic are in opposite directions, this harmonic is utilized in the backward wave oscillator. However, this property can cause oscillation in an amplifier unless some effort is made to suppress oscillations due to backward wave interaction.

Having found the modes of propagation, Sensiper solves for what can be called the characteristic impedance for these modes. The solution for the characteristic impedance is based on the expression

$$P_m = I_m^2 R_m$$

where $P_m$, the power flow along the helix, and $I_m$, the magnitude of the current along the tape, are due to the $m^{th}$ mode. $P_m$ and $I_m$ are computed from the field expressions by the usual methods. Fig. 10 is the equivalent circuit where the various $R_m$'s are associated with one particular propagating mode and are functions of ka. $Z_{local}(ka)$ is the impedance that represents the discontinuity in the local fields at the generator or point of excitation.

Fig. 11 shows the results of the calculations for several modes of the helix. The ordinate is equal to $R_m$ normalized with respect to the impedance of free space, $\sqrt{\mu/\epsilon}$. The $\beta_o$ mode in this figure corresponds very closely to what was called the zero mode in the sheath helix. Sensiper points out that although the mode impedances may be defined in several ways and although the actual currents which flow

through them will depend on the configuration of the source, these impedances at least indicate the relative ease with which the different waves are excited. It can be seen that for values of ka below approximately 0.7 all modes except $\beta_0$ have very high impedances. This indicates that these higher modes will be excited very little in this range of ka.

# CHAPTER III

# EFFECT OF SURROUNDINGS ON THE HELIX IMPEDANCE

## 1. General

The preceding analyses have assumed that the helix was surrounded by free space. In actual applications to traveling wave tubes the helix will be supported by a dielectric cylinder or by dielectric rods and may have a conducting shield surrounding portions of it. These surroundings will alter the phase velocity of the wave and the impedance of the helix, and hence, the gain of the tube. As will be pointed out later, the change in impedance can be used to good advantage in designing a matching system.

## 2. Sheath helix with dielectric surroundings

Pierce derives expressions for the effect of a dielectric on the transverse impedance and interaction impedance [8]. These expressions are based on the change in the propagation constant $\beta$ due to dielectric loading along an equivalent transmission line with distributed constants $X_L$ and $B_C$. If $B_C$ is increased by dielectric loading, the propagation constant $\beta$ will be increased to some larger value $\beta_d$. The original transverse characteristic impedance $K_t$ will then have a smaller value, $K_t'$ given by

$$K_t' = (\beta/\beta_d)\, K_t .$$

Now if $\beta/k$ is large so that $\beta_d \cong \gamma_d$ the axial interaction impedance will be decreased as follows:

$$\left[\frac{E^2}{\beta^2 P}\right]_d = \frac{\beta}{\beta_d}\left[\frac{I_0(\beta a)}{I_0(\beta_d a)}\right]\frac{E^2}{\beta^2 P} .$$

The factor $(\beta/\beta_d)$ is due to the reduction of impedance measured at the surface of the helix and the other factor is due to the greater falling off of the field toward the center of the helix because of the larger value of $\beta_d$. The actual phase constant with the helix mounted in its supports may be determined experimentally and knowing this the computed free space values of $K_t$ and $E^2/\beta^2 p$ may be altered to account, for the surroundings.

An analysis of the effect of an infinite dielectric surrounding on the phase velocity for the case of the sheath helix has been made by Harris [2] . The results of his investigation for a dielectric constant of 4.5, the average value for glass, are shown in Fig. 12. It can be seen that the phase velocity is lowered and caused to be more constant over a wider range of ka. For a helix mounted in a thick glass tube, these curves could be used to obtain a propagation constant for use in the expressions given in the previous paragraph in lieu of experimental values.

### 3. Sheath helix with inner or outer conducting shield

A conducting cylinder placed inside or outside a helix will appreciably alter its characteristics. G. W. Mather and G. S. Kino have made an analysis, using methods similar to those of Pierce, of the effect of internal and external shields on a sheath helix model. [6] . The same boundary conditions are imposed at the sheath and in addition the tangential electric field and the normal magnetic field at the conducting shields are made zero. The case of the external shield alone, as shown in Fig. 13, is the more important and will be discussed here. Cylindrical symetry is assumed as before and the wave equation is solved subject to

these boundary conditions. From these solutions curves are drawn for various values of b/a to show the effect on helix characteristics.

Fig. 14 shows the effect of the shield on the dispersion characteristics of the sheath helix. It is evident that the addition of the outer shield tends to make the phase velocity more constant and close to the asymptotic value of $v = c \sin\psi$ over a much larger range of frequency, i.e., $ka \cot\psi$ . It can be seen that the shield must be fairly close to the helix to have an appreciable effect. Due to the radial dependency of the fields the shield is more effective at lower frequencies where the fields extend out further.

An input impedance is defined on a current-power basis from the relation $Z_o = 2P/II^*$ using the current in the helical sheath and the power flow as found by integrating the Poynting vector over a cross section. For a perfect match to a coaxial line, the power flowing down the helix must equal the power flowing in the coaxial line. However, since the helix current does not equal the shield current, the difference being the displacement current within the helix, the choice of helix current is arbitrary and the impedance thus defined is not strictly an input impedance. Fig. 15 shows the normalized results for various values of b/a. It is apparent that for a close spaced shield the impedance is lowered considerably and is nearly constant over a large frequency range making it easy to match to a coaxial line. However, since a close spaced shield also lowers the longitudinal electric field, and hence, lowers the interaction impedance, a shield cannot be used for any considerable length along the helix or the gain of the tube will be seriously

reduced. Therefore, some type of transition is required from the low impedance shielded section used for matching to the high impedance section required for gain. These transitions will be discussed in Chapter IV.

4. Tape helix surrounded by an infinite dielectric

The case of a tape helix model surrounded by an infinite dielectric has been analyzed by P. K. Tien /12/. His approach is similar to that used by Sensiper for a tape helix in free space. To account for the effect of the dielectric upon the propagation constants he used the expressions developed by Harris which were based on the sheath helix. The results of this analysis are used to make comparisons to the sheath helix in free space. The value of the interaction impedance for free space is modified by two reduction factors, $F_1$ and $F_2$, where $F_1$ is the dielectric reduction factor and $F_2$ is the space harmonic reduction factor. The dielectric reduction factor is the reduction due to the decrease in phase velocity and modification of the fields due to the dielectric. The space harmonic reduction factor is the ratio of the power carried in the desired harmonic to the total power flow along the helix. The total impedance reduction factor, $F = F_1F_2$, is plotted as a function of the dielectric loading factor which is defined as the ratio of the phase velocity with no dielectric to the phase velocity with the dielectric present. The dielectric loading factor can be determined experimentally for any given helix and then F can be found from the curves. Tien's analysis does not consider the effect of the dielectric on the various mode characteristic impedances that are defined by Sensiper.

5. Impedance of a shielded helix based on distributed constants

Using an approach based on a distributed capacitance and an approxi-

mate velocity of propagation, C. C. Lund computes a characteristic impedance for a shielded helix [4]. He assumes that the distributed shunt capacitance is the same as for a coaxial line with an inner conductor of the same diameter as the helix and that the velocity of propagation is that given by waves traveling in the helical direction with the velocity of light. Then the $Z_o$ of the helix is derived as follows:

$$Z_o = \sqrt{L/C}$$

$$v = 1/\sqrt{LC}$$

$$Z_o = 1/CV = 1/C_{coax} \; c \sin \psi$$

Lund states that the value of v approximated this way checked very closely with measured values for helices of various pitch angles. As the author points out, the results probably are not accurate for an actual helix where the field distribution between the helix and the outer conductor are considerably different than that for a coaxial line. For helices with small pitch angles and close spaced shields these errors are probably small. His experimental results, obtained with a long tapered helix transition, indicate that the impedance computed in this manner is a good approximation to the actual value.

## 6. Experimental Results

A certain amount of work has been carried out in the measurement of the input impedance to the helix. This measured input impedance not only would include the characteristic impedance; but also the effect of the junction from one system to the other. Kraus has done a considerable amount of work in the analysis of the characteristics of the helical antenna and the input impedance of the helical antenna [3]. While

studying the helical antenna, Kraus made measurements which, in some cases, were for helices which were in the transmission line range of parameters. It was found that for values of ka below approximately 0.7 the input impedance was resistive, and had a value between 100 and 200 ohms. For values of ka above approximately 0.7 the impedance was found to be very sensitive to changes in frequency, and similar to the input impedance for a mismatched transmission line. It was found that the shape of the transition while having some effect did not alter the general shape of the impedance variation.

## 7. Summary

In analyzing the usefulness of the various methods used to define helix characteristic impedance, it is important to remember that each of these methods is somewhat arbitrary. The definitions based upon the distributed circuit constants are arbitrary due to the fact that inductance and capacitance are hard to define accurately at the microwave frequencies. The impedance based upon the helix fields is arbitrary because the selection of the characteristic component of electric field is arbitrary. The characteristic component of electric field is arbitrary. The characteristic impedance based upon the distributed circuit constants would seem to be more useful in qualitative work to indicate some of the important factors which determine the helix characteristic impedance.

Among the several definitions based on the helix fields it would be hard to select the most realistic one. The power-current impedance seems very realistic from low frequency concepts of current flow. For microwave applications this approach neglects the displacement current which would cause an error in most cases. The impedance based upon the

transverse voltage approach is similar to the normal transmission line terminal voltage convention. As we have seen, Pierce used this reasoning in his comparison of the results based on the transverse electric fields and the results based on the transmission line approach. Pierce used this approach to determine the effect of finite wire size on the actual helix characteristics. Generally speaking, the impedance analysis based upon the tape helix would seem to be the most promising from the standpoint of the model used. The greatest drawback to this analysis is the complexity of the expressions involved.

# CHAPTER IV

# METHODS OF COUPLING BETWEEN TRANSMISSION LINE AND HELIX

## 1. General

The criteria stated in the Introduction determine the general requirements for a transition from a conventional transmission line to the helix of a traveling wave tube. Obviously, a traveling wave tube can be only as good as the coupling that can be obtained between the two systems. The problem of coupling from a coaxial line or wave guide to a helix which is inside a glass envelope can be very difficult. The particular type of coupling used will depend a great deal on the specifications of the tube, e.g., the bandwidth, the physical dimensions, the power requirements, and the weight and space limitations. In this chapter some of the more common types of transitions used in traveling wave tubes will be discussed.

## 2. Waveguide coupling

One of the earliest types of coupling systems was the rectangular waveguide system shown in Fig. 16. The helix is terminated in a probe which extends through the waveguide and excites the $TE_{01}$ mode. The system may be tuned for best results across the band by adjusting the sliding short. This system is relatively narrow band in comparison with some of the other systems used. It also requires more space and weight and presents a difficult problem in design of the focusing magnet, but where these features are not important this system is quite satisfactory.

## 3. Cavity coupling

This system was also one of the first types to be used and is still used to a considerable extent. The cavity as shown in Fig. 17 is essentially a foreshortened coaxial cavity but it is much smaller than a

resonant cavity would be at the operating frequency of the tube. Its action is more in the nature of an impedance transformer. The extended center conductor of the coaxial line couples to the magnetic field of the cavity and in turn the straight probe on the helix is coupled by the magnetic field. The short cylinder attached to the end of the helix acts as a choke and helps to prevent radiation in the backward direction. The size of the cavity and the position of the probes can be adjusted by cut and try methods to give the best match. Normally a bandwidth of 2 to 1 may be obtained with this type of transition in the L and S bands. However, it is more difficult to make and adjust than some of the more recent types, and hence, its use in large scale production is decreasing.

### 4. Tapered transitions

This is a broad classification for a group of transition types which taper one or more dimensions to achieve a broadband impedance match between a transmission line and the helix. In the helix itself the turns per inch, wire size, or radius of the helix may be tapered, or, if there is an outer shield, this may be tapered in radius or shape. The theory for tapered lines shows that for an optimum match the rate of change of impedance per wavelength should be minimized. For short tapers an exponential taper is the best while for longer sections the so called "cosine" taper gives the best results [4]. In the exponential taper the impedance along the taper, Z(z), is made to vary in the following manner

$$Z(z) = Z_1 \, e^{(z/\ell)(\log Z_2/Z_1)}$$

where $Z_1$ and $Z_2$ are the initial and final impedances, $\ell$ is the electrical length of the taper, and z is the distance along the axial coordinate measured in electrical degrees. The impedance in the cosine taper

obeys the following function

$$Z(z) = Z_1 \, e^{-\frac{1}{2}\log(Z_2/Z_1)\cos(\pi z/\ell)}$$

Knowing Z(z) the variation of dimensions required to give this function may be computed using one of the methods given in the previous chapters. In many applications, however, practical considerations require a linear taper. In any case, for a broadband transition, the taper should be over one half wave length long.

A tapered transition developed by C. O. Lund is based on a change in the helix pitch which is made to vary so that the impedance of the transition follows the cosine function mentioned above. The transition is made between a helix with an outer shield to a coaxial line with an inner conductor the same radius as the helix as shown in Fig. 18. While this system gives an excellent match, it has several mechanical drawbacks; it requires precision milling of the transition and helix from a metal cylinder and a coaxial cathode and collector arrangement. These factors limit it to relatively low frequency tubes with large helices. In addition the external shield lowers the interaction impedance which reduces the gain per wavelength.

One form of tapered helix that is sometimes used in conjunction with waveguide or cavity coupling to reduce the discontinuities as well as improve the impedance match is the exponential taper. In this form the helix pitch is tapered approximately exponentially without attempting to calculate a precise function which the helix impedance should follow. It is assumed that if the helix pitch varies exponentially, then the helix impedance will also vary exponentially. If the standard pitch of the helix is $p_0$ as shown in Fig. 19, then the distance z from

the origin to the end of the $n^{th}$ turn is given by

$$z = \int_0^n p_o e^{mn} dn$$

or

$$z/p_o = (e^{mn} - 1)/m$$

where m is a constant which determines the exponential rate of change of pitch. Tables of $(e^{mn} - 1)/m$ have been computed for various values of m for n up to ten turns. The tables are used to calculate the distance which the lathe carriage must be manually advanced between each turn when winding the transition sections at each end of the helix.

A type of tapered transition based on a tapered conducting shield has been mentioned and will be discussed in Chapter V.

5. Stub compensated transitions

Measurements of helix impedance by E. R. White, using a long tapered pitch transition section, indicate that over quite a wide frequency range the helix impedance may be represented by a series RLC circuit with the magnitude of the resitive component being relatively large /14/. An impedance of this kind may be transformed to a normalized value near $1+j0$ over a fairly broad band by a combination of a line transformer and a parallel or series transmission line section. Fig. 20 shows the equivalent circuit and a possible arrangement for the matching section in the parallel case.

Here $Z_h$ represents the measured impedance of the helix, $\ell_1$ a length of transmission line of characteristic impedance $Z_o$ connected in series between the input terminals and the helix, and $\ell_2$ a short circuited length of transmission with the same $Z_o$ connected in parallel at the junction of the input terminal and the line section. Assuming negligible

attenuation the input impedance of the network is given by

$$Z_{in} = \frac{Z_o^2 \tan\beta\ell_1 \tan\beta\ell_2 - jZ_oZ_h \tan\beta\ell_2}{Z_h \tan\beta\ell_1 \tan\beta\ell_2 - Z_h - jZ_o \tan\beta\ell_2}$$

This can be solved for various values of $\beta$ , $\ell_1$, $\ell_2$, and $Z_o$ by use of a Smith chart, and, by a series of successive approximations, appropriate values for these terms can be found which will give the desired input impedance. In general, with this type of transition bandwidths of two to one are obtainable. Since the long drift tube adds appreciably to the overall length of the tube, a modification using a strip line technique as shown in Fig. 21 has been developed by White.

6. Coupled helix transitions

One of the more promising systems of coupling to a helix is by the use of coupled helices /5,7,13/. The primary advantage of the coupled helix system is that it can be completely external to the vacuum envelope and still effectively couple r.f. energy through the glass walls. Another advantage is the fact that the outer helix and shield does not appreciably affect the usefulness of the inner helix for interaction purposes. In addition the multielement configurations, tapers, or direct vacuum leads of other systems are replaced by a simple constructed helix with an outer shield. The arrangement which is generally used is shown in Fig. 22. Experimental work that is normally time consuming and expensive becomes simply a matter of slipping couplers on and off. Since the traveling wave tube is not limited to amplifiers, input and output couplers may be placed at will along the tube to try various multiplier and mixer combinations.

The basic phenomena involved is that of spatial beating between coupled transmission lines. Transmission line theory shows that when two infinitely long helices are coupled in such a manner that the inductive and capacitive couplings are equal, we have the exact analog of two coupled pendula. In the same manner that energy is transferred from one pendulum to the other and back as time increases, so energy is transferred from outer to inner helix and back as axial distance is increased. The beat wavelength $\lambda_b$ is defined as the axial distance required to transfer energy from one to the other and back. Similarly, the beat phase constant may be defined as $\beta_b = 2\pi / \lambda_b$.

The analysis presented here follows that given by O. G. Owens [7] which is based in part on Pierce [8]. Consider two infinitely long concentric helices where helix no. 1 is the outer helix and helix no. 2 is the inner helix, which have the following distributed constants; series impedances $jX_1$ and $jX_2$ , shunt admittances $jB_1$ and $jB_2$, and are coupled by series mutual impedance $jX_{12}$ and shunt mutual admittance $jB_{12}$. Assuming a single traveling wave in the direction of positive z which varies as $e^{j(\omega t - z)}$, then the following standard transmission line equations apply

$$\Gamma I_1 - jB_1V_1 - jB_{12}V_2 = 0$$

$$\Gamma V_1 - jX_1I_1 - jX_{12}I_2 = 0$$

$$\Gamma I_2 - jB_2V_2 - jB_{12}V_1 = 0$$

$$\Gamma V_2 - jX_2I_2 - jX_{12}I_1 = 0$$

Solving these for $\Gamma$ and defining an inductive coupling coefficient

$$q_L = X_{12} / \sqrt{X_1X_2}$$

and a capacitive coupling coefficient

$$q_C = B_{12} / \sqrt{B_1 B_2}$$

and assuming that the helices are constructed to have equal phase velocities such that $X_1 B_1 = X_2 B_2 = -\beta^2$

we obtain

$$\Gamma^2 = \beta^2 \left[ 1 + q_L q_C \pm (q_L + q_C) \right]$$

If the helices are wound in opposite directions, i.e., if the inner helix is wound as a right hand screw, the outer helix is wound left hand, and if $qL = q_C$, then complete power transfer takes place. Substitution of $q = q_L = q_C$ and selection of the positive root gives

$$\Gamma^+ = \beta(1 + q)$$

$$\Gamma^- = \beta(1 - q)$$

Thus there are two modes traveling at different velocities in the positive direction which can aid or oppose one another and produce beats along the length of the double helix combination.

Owens shows that when one line only is excited ahead of the point where it couples to a finite properly terminated second line, the two modes set up in the first line are equal, i.e., at $z = 0$, $V_1^+ = \frac{1}{2}V = V_1^-$ Pierce shows that for the synchronous case, i.e., $X_1 B_1 = X_2 B_2$, the corresponding mode voltages are equal in magnitude, $V_1^+ = V_2^+$ and $V_1^- = -V_2^-$

Expressions for the total voltages on either helix can now be written

$$V_1 = \tfrac{1}{2}V\, e^{j[\omega t - \beta(1 + q)z]} + \tfrac{1}{2}V\, e^{j[\omega t - \beta(1 - q)z]}$$

$$= V\, e^{j(\omega t - \beta z)} \cos q\beta z$$

and

$$V_2 = \tfrac{1}{2}V\, e^{j[\omega t - \beta(1 + q)z]} - \tfrac{1}{2}V\, e^{j[\omega t - \beta(1 - q)z]}$$

$$= -jV\, e^{j(\omega t - \beta z)} \sin q\beta z$$

A plot of $V_1$ and $V_2$ is given in Fig. 23. The envelopes of $V_1$ and $V_2$ correspond to cos $q\beta z$ and sin $q\beta z$ respectively. The quantity $\delta_b = q\beta$ may be termed the beat phase constant.

The relation between q and $\beta$ is developed as follows. Assume that the radii of the inner and outer helix are a and b respectively and that the signal on the inner helix is zero at the transverse plane $z = a$, while at plane $z = e$ the signal on the outer helix is zero. The longitudinal component of electric field $E_z$ is derivable from the voltage in a single helix as $E_z = -\partial V/\partial z = \Gamma V$. At the planes $z = d$ and $z = e$ the field distribution can be considered as due to one helix since the signal is zero on the other one. Let $E_{zad}$ denote the value of $E_z$ at radius a in the plane $z = d$ and other symbols to correspond. Remembering that $I_1 = 0$ at $z = d$ and $I_2 = 0$ at $z = e$ the transmission line equations involving $\Gamma V_1$ and $\Gamma V_2$ can be written at plane $z = d$.

$$E_{zad} = \Gamma V_1 = jX_{12}I_2$$

$$E_{zbd} = \Gamma V_2 = jX_2I_2$$

and at plane $z - e$

$$E_{zae} = \Gamma V_1 = jX_1I_1$$

$$E_{zbe} = \Gamma V_2 = jX_{12}I_1$$

then dividing

$$\frac{E_{zad}}{E_{zbd}} = \frac{X_{12}}{X_2}$$

$$\frac{E_{zae}}{E_{zbe}} = \frac{X_1}{X_{12}}$$

Dividing the first by the second and replacing the $E_z$ terms by their Bessel function equivalents as given by Pierce in Ref. 8 gives

$$\frac{X_{12}^2}{X_1 X_2} = \frac{I_o(\gamma a)\, K_o(\gamma b)}{I_o(\gamma b)\, K_o(\gamma a)}$$

The first term is merely $q_L^2$ so we have

$$q_L = q = {\frac{I_o(\gamma a)\quad K_o(\gamma b)}{I_o(\gamma b)\quad K_o(\gamma a)}}^{\frac{1}{2}}$$

At the frequencies of interest $\gamma \approx \beta$ and substituting the first terms of the asymtotic series for the $I_o$ and $K_o$ functions, a useful approximation is obtained

$$q \approx e^{-\beta(b-a)} \approx e^{-\beta a(b/a - 1)}$$

This is plotted in Fig. 24 for various values of b/a [13].

The presence of the grounded outer shield can be taken into account by use of an equation developed by G. S. Kino in an unpublished work

$$q = q_{ab}\sqrt{\frac{1 - q_{bc}^2}{1 - q_{ac}^2}}$$

where a, b, c = radii of the inner, outer, and shield respectively

$q$ = modified coupling coefficient

$q_{ab}$ = unmodified coupling coefficient between the helices

$q_{bc}$ = coefficient between the outer helix and shield as though the shield were an outer helix

$q_{ac}$ = coefficient between the inner helix and shield, ignoring the presence of the outer helix

The values of the various coupling coefficients may be determined from Fig. 24 and used in the above formula to find the modified coefficient.

From the first helix of Fig. 23 it is evident that for complete transfer of power from the outer to the inner helix, a quarter beat wavelength should be used, i.e., cos $q\beta\ell = 0$ or $q\beta\ell = \pi/2$. Both q and $\beta$ vary with frequency so perfect transfer cannot be achieved except at discrete frequencies for which $q\beta\ell = \pi/2$. But since $\beta$ increases with frequency and q decreases with frequency, appropriate selections of b/a and $\ell$ will give quite broad band operation. The upper curve of Fig. 25 shows the variation of $q\beta\ell$ with $\beta(b - a)$ plotted from the relation $q\beta\ell = \beta\ell\, e^{-\beta(b - a)}$ [5].

The general shape of this curve is the result of the variation of $\beta$ which is approximately linear with frequency and the decrease of q due to the pulling in of the fields at the higher frequencies. This shows that the length of the coupling helix may be adjusted so that $q\beta\ell$ passes through $\pi/2$ twice giving the double humped response indicated in the lower curve of Fig. 25. Owens shows that the optimum bandwidth is obtained if the maximum value of $q\beta\ell$ at $\beta(b - a) = 1$ is near $100^\circ$.

A recent report by G. Wade indicates that the presence of the electron beam modifies the behavior of the coupled helix transition substantially [13]. Calculated curves of power variation with length of the coupler show that beam interaction tends to prevent the possibility of complete power transfer between helices. As the tightness of the coupling between helices is increased the effect of the beam interaction decreases and the degree to which power may be transferred is increased.

Calculation also indicates that the proper length for input and output couplers is greater than the length for complete energy transfer between helices in the absence of the beam.

## CHAPTER V

## DESIGN OF PARTICULAR COUPLING SYSTEMS

### 1. General

This chapter will deal with the developement of the r.f. coupling system for a particular traveling wave tube, the Sylvania TWT No. 591. This is an X - band, 8 to 12.4 KMC, high power tube, designed for pulsed operation. The peak power output is one kilowatt with a .005 duty cycle giving an average power output of 5 watts. The collector is pulsed at 7000 volts to produce a peak beam current of about 1.5 amps. The final design will incorporate a control grid to perform the pulsing operation. The specifications call for demensions of 7 inches by one inch in diameter with only 3.5 to 4 inches for the helix, depending on the type of coupling used. The helix mean diameter is .090 inches; it is wound from .025 x .005 tungsten or molybdenum tape at 27 TPI. The specifications limit the total weight, including the focusing magnet, to 7 lbs. This presumes that a system of periodic focusing with permanent magnets can be developed. If this proves unfeasible, and a solenoid type magnet is required, a total weight of 35 lbs. will be allowed.

At present the developemental tubes utilize waveguide coupling since satisfactory coupling is obtained and the helix configuration for this type of coupling is relatively simple. However, waveguide coupling requires either large entrance holes through the focusing solenoid or the solenoid must have a large inner diameter to allow entry of the waveguide. Both arrangements result in heavier, bulkier magnets which require more power to operate and, of course, periodic focusing with

permanent magnets becomes impossible. Since the system in which this tube will be operated has severe limitations in regard to space, weight, and power, it is evident that some type of coaxial line coupling will be necessary. The writer was assigned the project of developing such a coupler. At that time, the only known successful type of coupling in this band was with waveguide. An SWR of 2 to 1 or better was specified.

## 2. Tapered shield transition

The first approach followed the method suggested by Mather and Kino of lowering the helix input impedance by enclosing it in a close spaced shield which is then tapered away radially to permit maximum strength of the axial electric field. A linear taper approximately two axial wavelengths in length at the center frecuency was selected for convenience. The axial wavelength of the unshielded helix may be determined from the dispersion curve of Fig. 14 for $b/a = \infty$ and the value of $\gamma$ obtained is used in the expression $\beta = \sqrt{\gamma^2 + k^2}$

From the given helix constants, at the center frequency $ka \cot\psi = 1.34$ which results in a value of $\beta = 25.2$ or $\lambda_h = .25$ inches. This means that the tapered section should be roughly .5 inches long and in that distance its radius should increase to a value such that b/a is effectively infinite. Now going to the power-current impedance curves of Fig. 15, it is seen that at $ka \cot\psi = 1.35$ any value $b/a > 3$ is effectively infinite. For mechanical reasons, the first choice for the smaller shield radius was 1.070", just slightly larger than the outer radius of the glass envelope. With $a = .045$ " and $b = .070$" the angle

required to give $\frac{b}{a} = 3$ in .5" is $9^{\circ}$. Fig. 26 is a sketch of the experimental transition. The tapered shield is split along the horizontal plane through the axis to allow assembly over the glass bead and tungsten pin.

Thus with the shield as close to the helix as the glass envelope will allow, i.e., $b/a = .070/.045 = 1.55$, the free space impedance of the shielded helix is found from Fig. 15 to be 84 ohms. Experimental measurement of the wavelength along the shielded helix with and without the glass dielectric present determined that the dielectric loading factor was about .65. Using this in Pierce's expression $K_d = \beta/\beta_d K$ gives an impedance of 55 ohms for the shielded helix in the glass envelope. As a check on this value the method used by Lund was applied. This states that the impedance of a shielded helix is approximately equal to the impedance of a coaxial line of the same dimensions multiplied by a factor $\lambda/\lambda_h$ where $\lambda$ is the wavelength in the coaxial line and $\lambda_h$ is the wavelength along the helix. From the standard formula for the impedance of coaxial line, $Z = (60/\sqrt{\epsilon})(\ln b/a)$, we have for $\epsilon = 4.5$ and $b/a = 1.55$, $Z_{coax} = 12.4$ ohms. At 10 KMC, $Z_{helix} = Z_{coax} \lambda/\lambda_h = 12.4 \times 1.18/.218 = 67$ ohms. These two values are in fairly close agreement and indicate that when the transition is connected to a 50 ohm line an SWR of about 1.3 is possible assuming no discontinuities and a perfect taper. With a thinner glass wall the ratio of b/a could be decreased and the helix impedance made closer to 50 ohms but no such tubing was available. As it was, it was extremely fragile at the pin seal. The impedance of the unshielded helix is found by use of Fig. 15 and the experimentally determined dielectric loading factor to be about 120 ohms at 10 KMC.

Hence, direct connection of the helix to a 50 ohm line would cause an SWR of 3 to 1 in at least portions of the band.

The coaxial line connection to the helix is designed to have a constant impedance of 50 ohms. The diameter of the sleeve connecting the center conductor to the tungsten pin and the diameter of the pin are selected so that the impedance as computed by the standard coaxial line formula remains constant as the dielectric changes from Teflon to air to glass.

The experimental helix models for testing the match were made by sealing a short tungsten pin in the glass tube, spot welding the helix to the pin, and terminating the helix with a coating of aquadag. Several models were made and tested but the results varied greatly, and all gave an SWR of more than 2 to 1 at some point across the band, particularly at the high end. Assuming that the trouble might be due to too great a taper angle, shields were made with tapers of $5^{\circ}$, $3^{\circ}$, and a rough exponential flare, but these gave no apparent improvement.

A new group of models were made and tested and, fortunately, some of them gave satisfactory results. Close examination under a microscope revealed that an imperfect welded joint between the helix and the pin could introduce discontinuities which had a considerable effect on the match that was obtained. A clean, solid weld with the pin exactly centered on the helix and no portion of the helix extending beyong the pin except in the direction of conduction always gave good results. Retesting of the good models with the various shields revealed that the $5^{\circ}$ taper gave slightly better results than the other angles.

A model with an input and output transition and a standard length,

3.5 inch, helix was made to test the transmission characteristics. These tests showed that the loss across the band was less than 0.5 db more than the computed cold loss for a helix of this length. The most favorable results are shown in Figs. 27 and 28. Very similar results were obtained with several other models. It is believed that the transition is easily reproducible as far as the electrical characteristics are concerned. However, it has several drawbacks of a mechanical nature; the pin seal is difficult to make, it is quite fragile because of the small size of the tube, and it is easily broken during assembly. Two attempts to make a complete tube using this system ended in failure due to breakage of the pin seal while assembling the transition section. Lack of time prevented further trials.

Some work was done on the matching section for a ruggedized, all metal version of this tube which is in the planning stage. As presently conceived, the helix will be braized to three sapphire rods for support and enclosed in a non-magnetic stainless steel envelope as shown in Fig. 29. This configuration will permit the shield to be brought as close to the helix as necessary to allow exact matching to the helix impedance. The value of b required to give an input impedance of 50 ohms may be computed from Fig. 15. In this case, the TPI of the helix is increased to 27 because the dielectric loading of the sapphire rods is less than that of glass tubing. The computed value of b is .053" which leaves only .006" clearance between the helix and shield. A $5^{\circ}$ tapered shield was used as in the previous system. Several models were made and tested and gave fairly good results, but as before, it seemed that the discontinuity at the junction of the center conductor

and helix was causing considerable reflections. Moving the hole for the coaxial line off center permitted the center conductor of the coax to join the helix tangentially, thereby reducing the source of discontinuity. This configuration, which is the one shown in Fig. 29, improved the match substantially. The results obtained are given in Fig. 30 and 31.

### 3. Coupled helix transition

The mechanical disadvantages of the tapered shield transition as used with the glass vacuum envelope are absent in a coupled helix transition. However, there is a greater insertion loss, the magnitude of which is determined by the degree of coupling obtainable through the glass walls.

The first step in the design of the coupler is to determine the TPI required in the outer helix to give the same phase velocity as the main helix at the high frequency end of the band. This is done because the coupling between the two helices decreases with frequency, and hence, any initial phase velocity difference has more effect at higher frequencies. This TPI can be computed approximately by considering the helices in free space since they will both be affected similarly by the dielectric and the shield. The exact matching of velocities for best results will require a cut and try process so more accurate information is not necessary. Using Fig. 14 and the mean diameter of the outer helix, .068", the TPI required was computed to be 11.5.

The next step is to compute the spacing between the outer helix and the shield required to match the input impedance of this helix to a 50 ohm coaxial line. From Fig. 15 this was determined to be .088". Next the required length of coupler is computed from the expression $\cos q\beta\ell = 0$ which was explained in Chapter IV. This is also computed at the high

frequency end since this gives the largest value for $\ell$ . The optimum value of $\ell$ is best found by making the outer helix slightly longer than the computed value and then trimming it turn by turn until the best match is obtained. The computed value of $\ell$ gave about 6 turns for the outer helix.

Then by a tedious process of cut and try, the optimum values for the number of turns and the TPI was found to be 4½ and 13 respectively. This gave the results shown in Fig. 32 and 33. The higher insertion loss was not considered excessive for this tube. A tube using this type of transition was in the process of being tested when time ran out.

## 4. Conclusions

Among the transitions discussed in this work, the coupled helix system is undoubtedly the most desirable from a construction standpoint as far as glass tubes are concerned. It does have a higher insertion loss than some other types and for this reason may prove to be unsatisfactory for high power tubes. In this case the tapered shield transition merits consideration in spite of its mechanical disadvantages.

Since completion of the above work on transitions, one of the large electronics concerns has announced an X-band tube which uses the strip line, stub compensation technique in an all metal construction. Their published curve of SWR is slightly better than that obtained for the tapered shield system in an all metal tube. Further work will be required to determine which system is superior.

# BIBLIOGRAPHY

| | | |
|---|---|---|
| 1. | C. C. Cutler | EXPERIMENTAL DETERMINATION OF HELICAL WAVE PROPERTIES, Proceedings of the I.R.E. - February, 1948 |
| 2. | Harris, Johnson, Darp, and Smullin | SOME MEASUREMENTS OF THE PHASE VELOCITY ALONG A HELIX WITH DIELECTRIC SUPPORTS, M.I.T. R.I.E. Report No. 93 |
| 3. | Kraus and Glasser | MEASURED IMPEDANCE OF HELICAL BEAM ANTENNAS RADIATING IN THE AXIAL MODE, Journal of Applied Physics - February,1948 |
| 4. | C.O. Lund | BROADBAND TRANSITION FROM COAXIAL LINE TO HELIX, RCA Review, March, 1950 |
| 5. | P. Lacy | APPLICATIONS OF COUPLED HELICES, Presented to West Coast Convention of I.R.E., August, 1953 |
| 6. | G.W.Mathers and G.S. Kino | SOME PROPERTIES OF A SHEATH HELIX WITH A CENTER CONDUCTOR OR EXTERNAL SHIELD, Stanford University E.R.L. Technical Report No. 65, June 17, 1953 |
| 7. | O.G. Owens | COUPLED HELIX ATTENUATORS FOR TRAVELING WAVE TUBES, Stanford University E.R.L. Technical Report No. 68 |
| 8. | J.R. Pierce | TRAVELING WAVE TUBES, D. Van Nostrand Co. Inc. New York, 1950 |
| 9. | J.R. Pierce | THEORY OF THE BEAM TYPE TRAVELING WAVE TUBE, Proceedings of the I.R.E., February, 1947 |
| 10. | S. Sensiper | ELECTROMAGNETIC WAVE PROPAGATION ON HELICAL STRUCTURES, Proceedings of the I.R.E., February, 1955 |
| 11. | S. Sensiper | ELECTROMAGNETIC WAVE PROPAGATION ON HELICAL CONDUCTORS, M.I.T.R.L. Electronics Technical Report No. 194, May, 1951 |
| 12. | P.K. Tien | HELIX IMPEDANCE OF TRAVELING WAVE TUBES, Stanford University E.R.L. Technical Report No. 50, June 1952 |
| 13. | G. Wade and N. Rynn | COUPLED HELICES FOR USE IN TRAVELING WAVE TUBES, Unpublished report of Stanford University E.R.L. February,1955 |
| 14. | R.E. White | COAXIAL TO HELIX TRANSDUCERS FOR TRAVELING WAVE TUBES, Presented to I.R.E. National Convention,N.Y.,N.Y.,March,1953 |

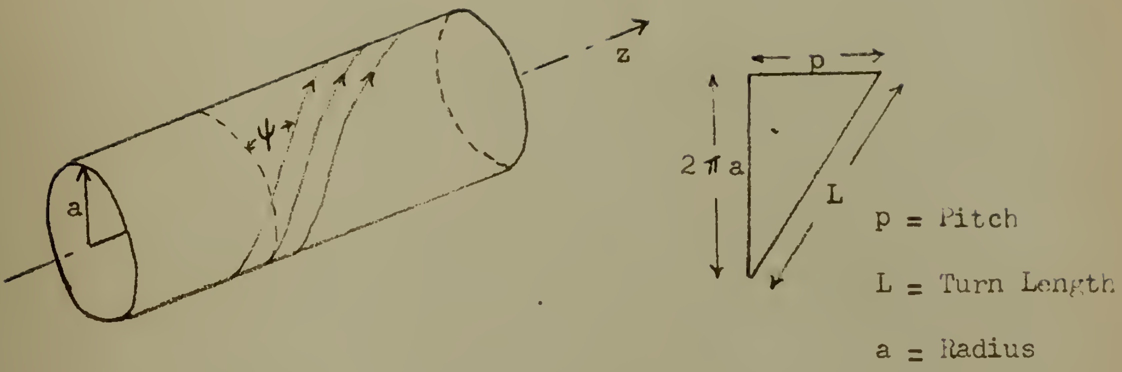

Fig. 1. Sheath helix model

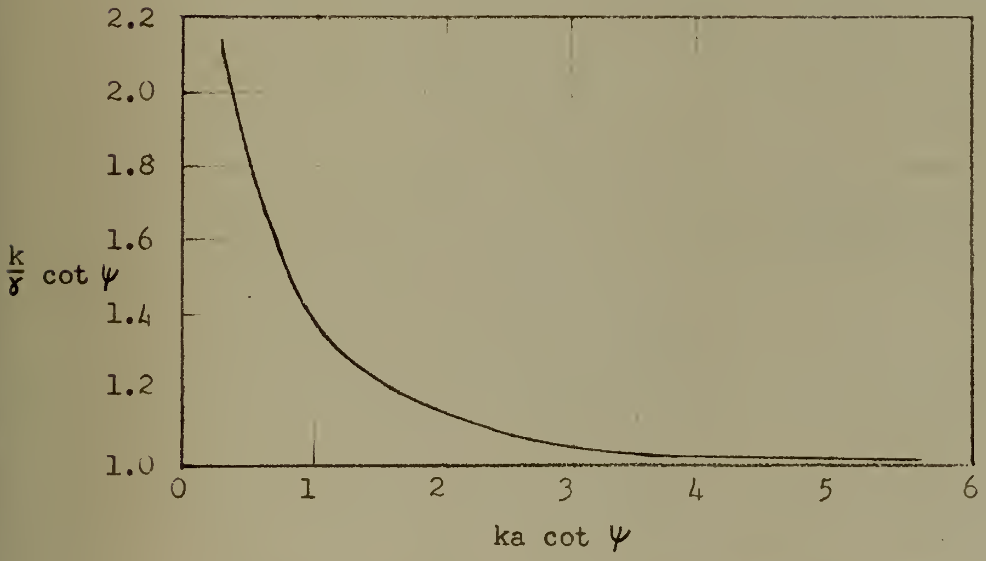

Fig. 2. Dispersion curve of the sheath helix

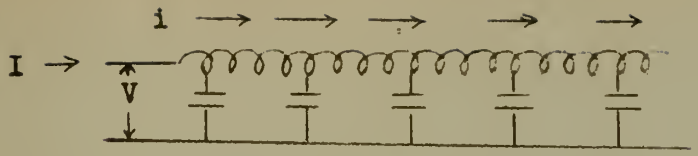

Fig. 3. Equivalent Circuit for helix

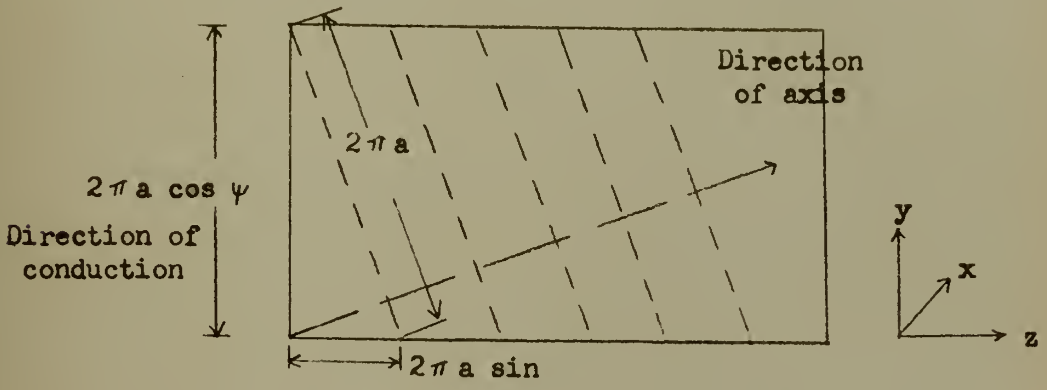

Fig. 4. Developed sheath helix model

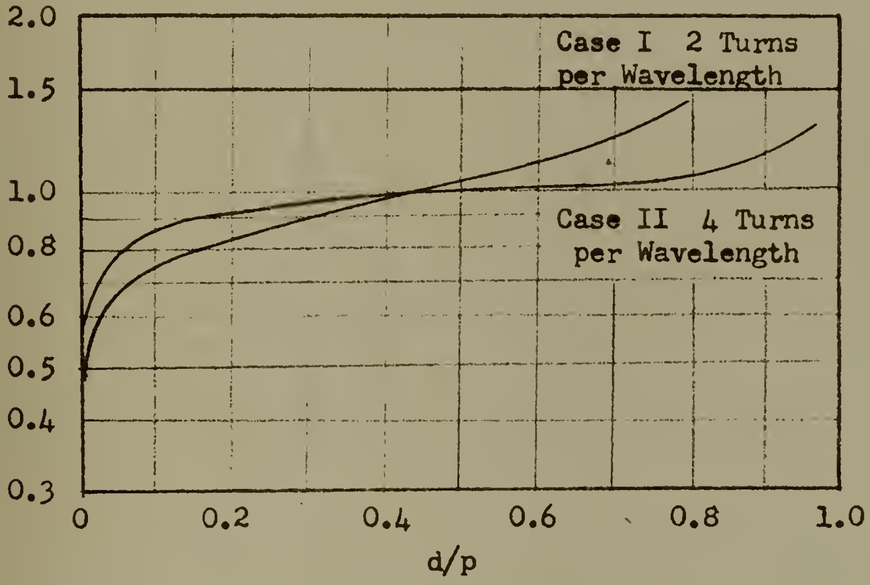

Fig. 5. Effect of wire size on interaction impedance

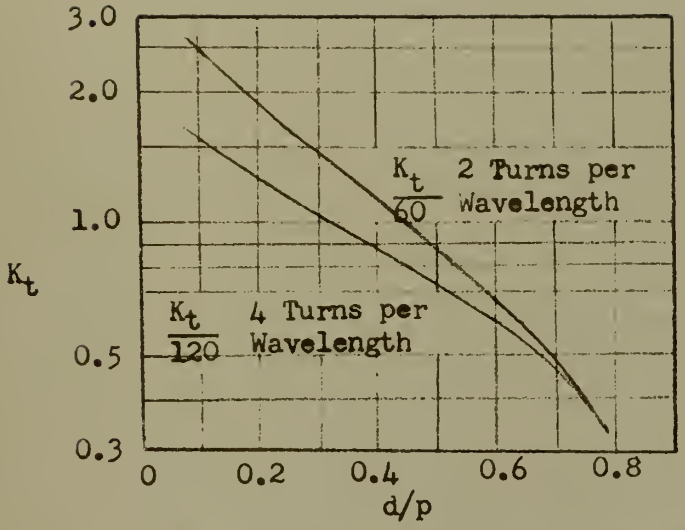

Fig. 6. Effect of wire size on transversed impedance

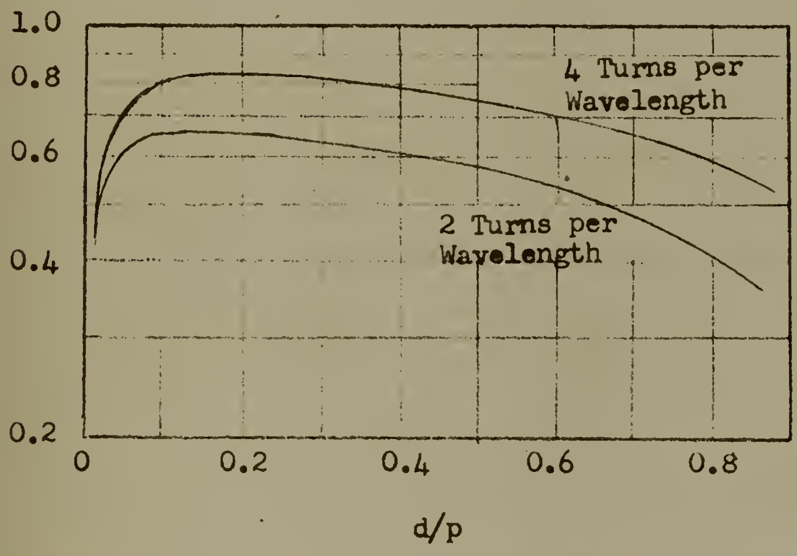

Fig. 7. Ratio of interaction impedance at longest allowable radius to interaction impedance at surface of developed sheet

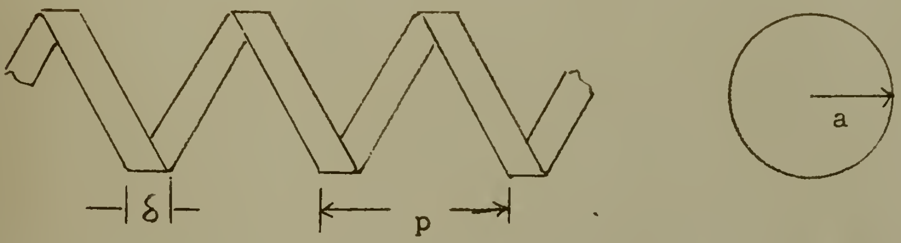

Fig. 8. Tape helix model

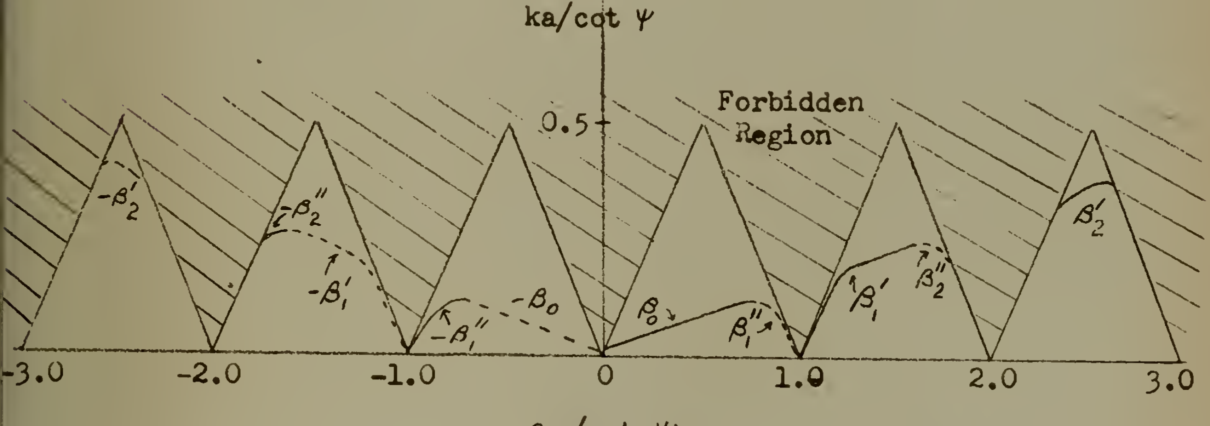

Fig. 9. Propogation constants of tape helix model

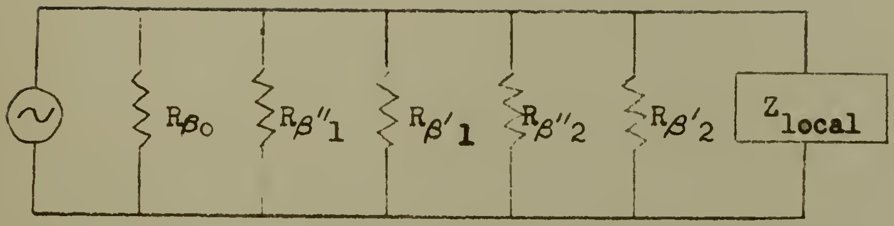

Fig. 10. Equivalent circuit of tape helix mode.

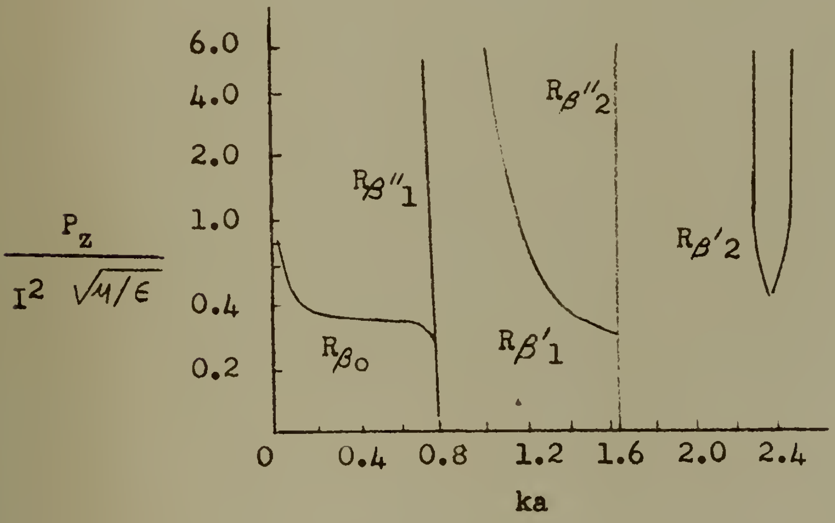

Fig. 11 Mode impedances of tape helix model

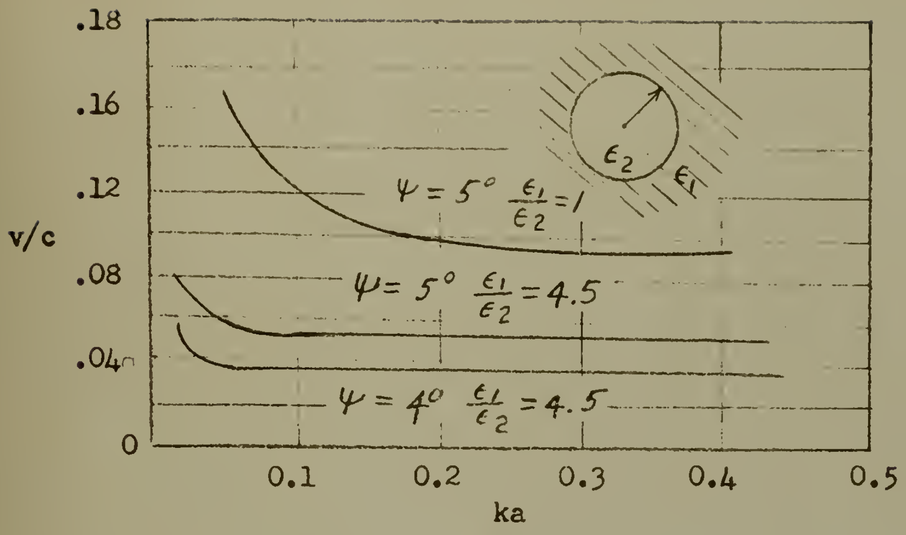

Fig. 12. Effect of dielectric on sheath helix

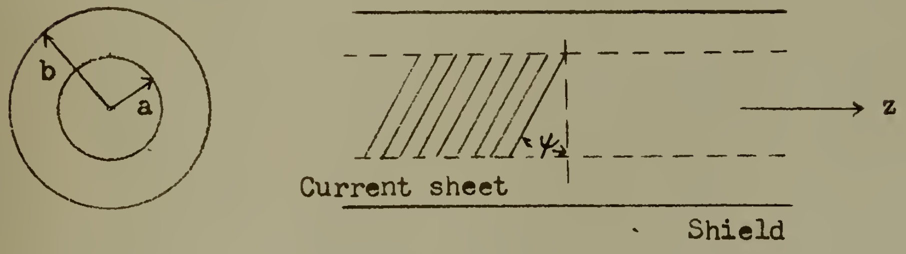

Fig. 13. Sheath helix with external shield

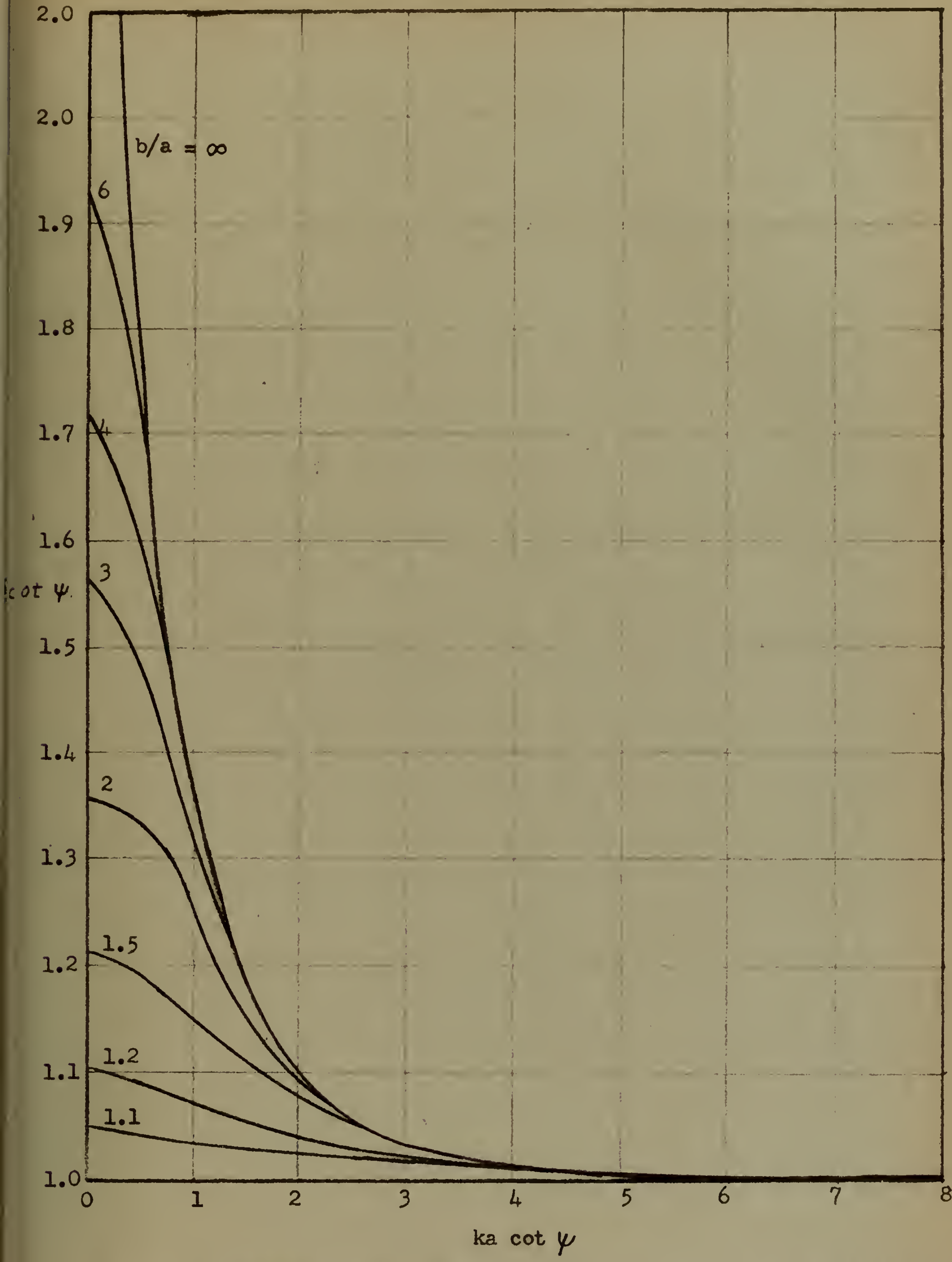

Fig. 14. Dispersion characteristics of sheath helix with external shield

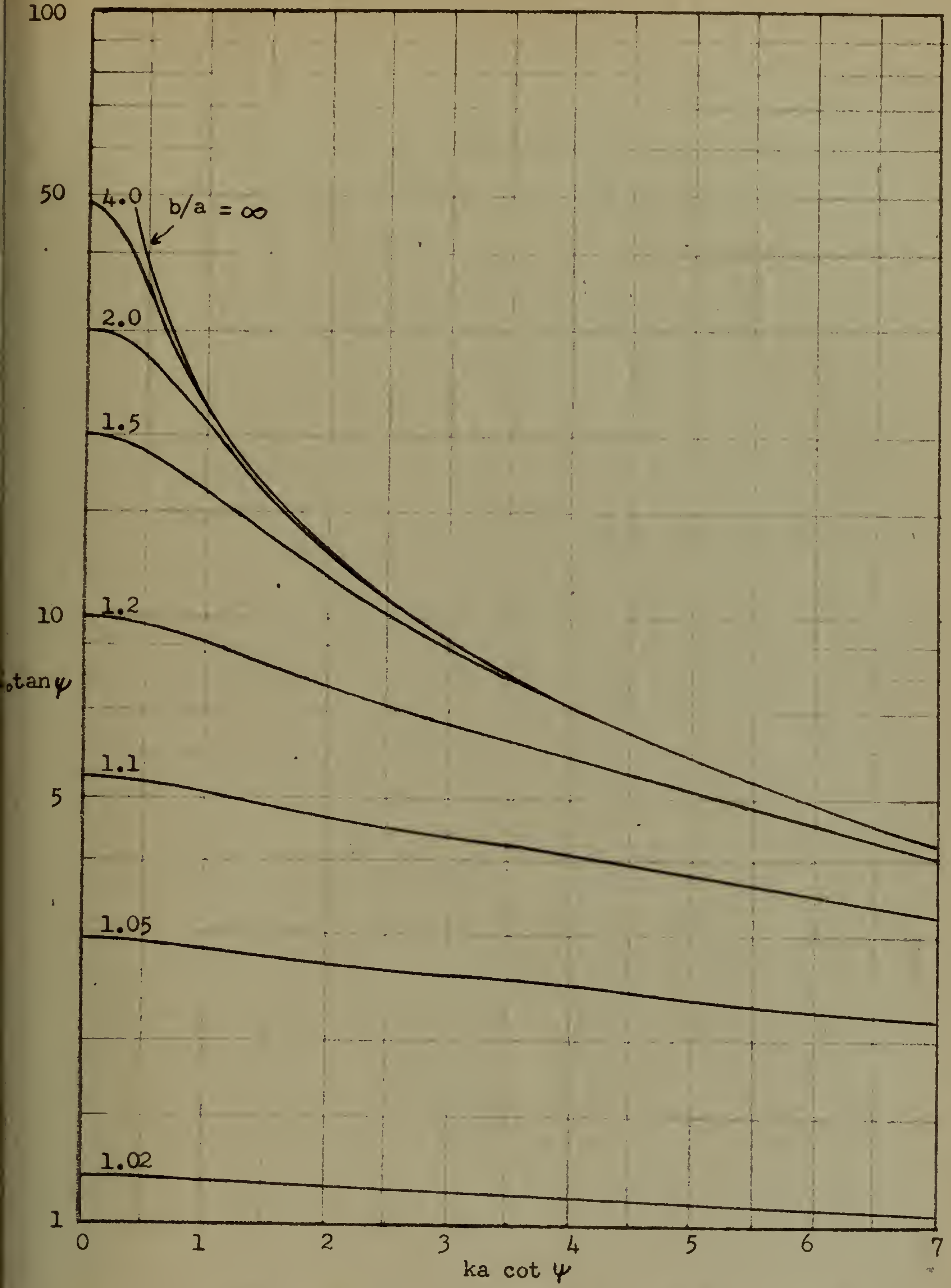

Fig. 15. Power-current impedance factor for sheath helix with external shield

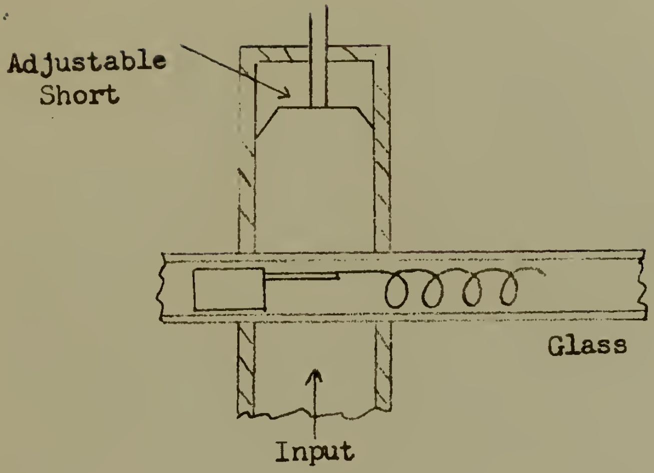

Fig. 16. Rectangular waveguide coupling

---

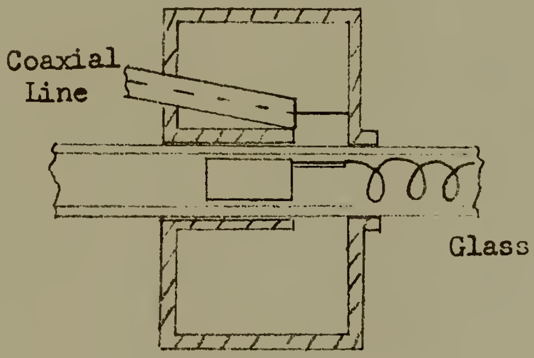

Fig. 17. Cavity coupling system

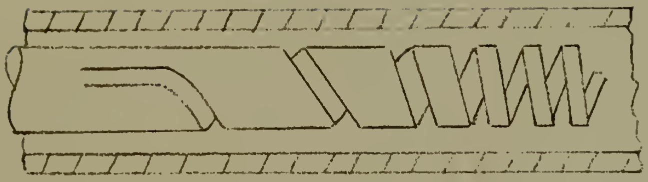

Fig. 18. Tapered helix with external shield

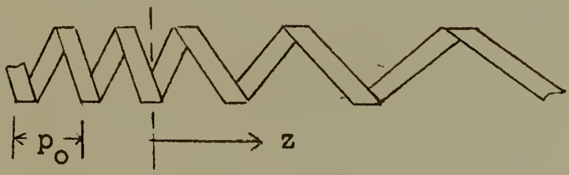

Fig. 19 Helix with tapered pitch

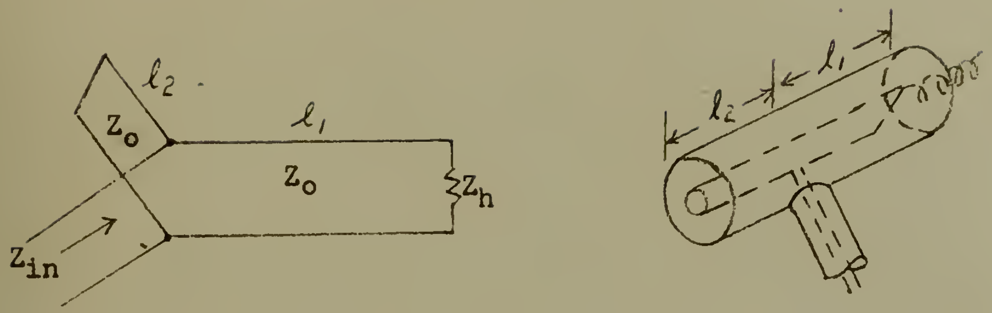

Fig. 20. Equivalent circuit and configuration for stub compensated transition

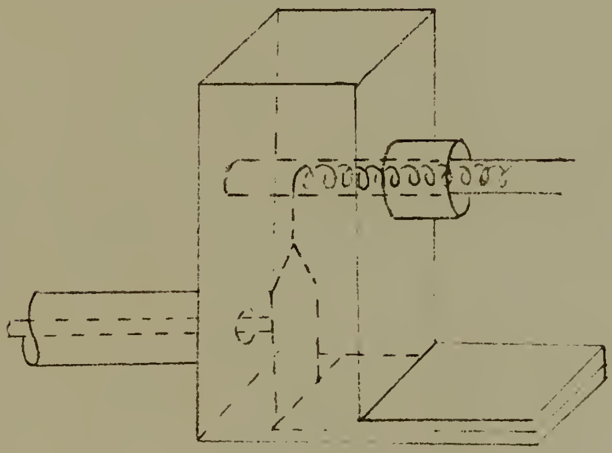

Fig. 21. Configuration for stub compensated transition using strip line technique

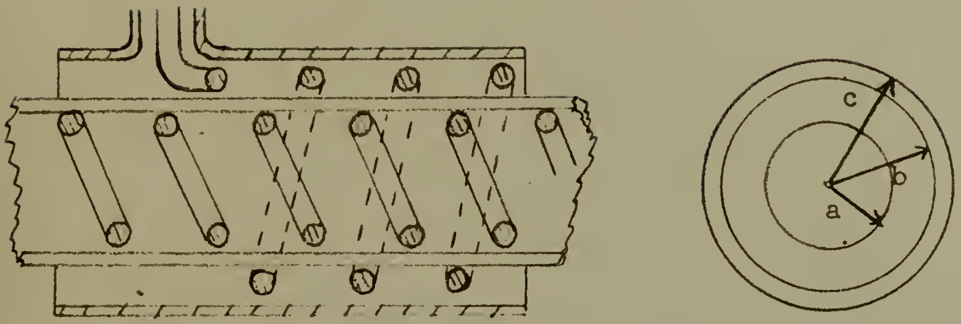

Fig. 22. Coupled helix transition

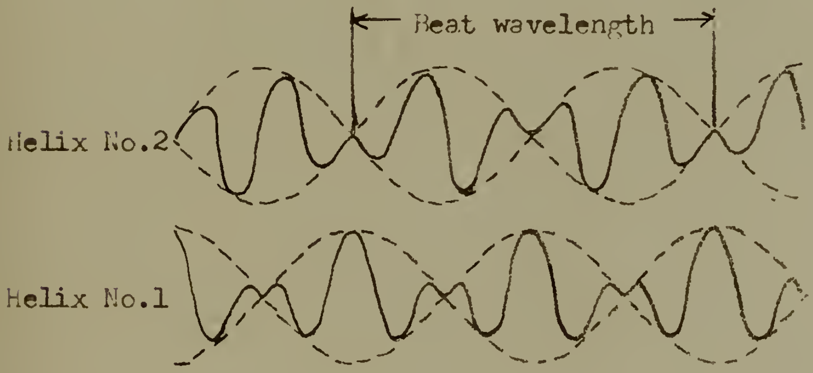

Fig. 23. Voltage variation along coupled helices

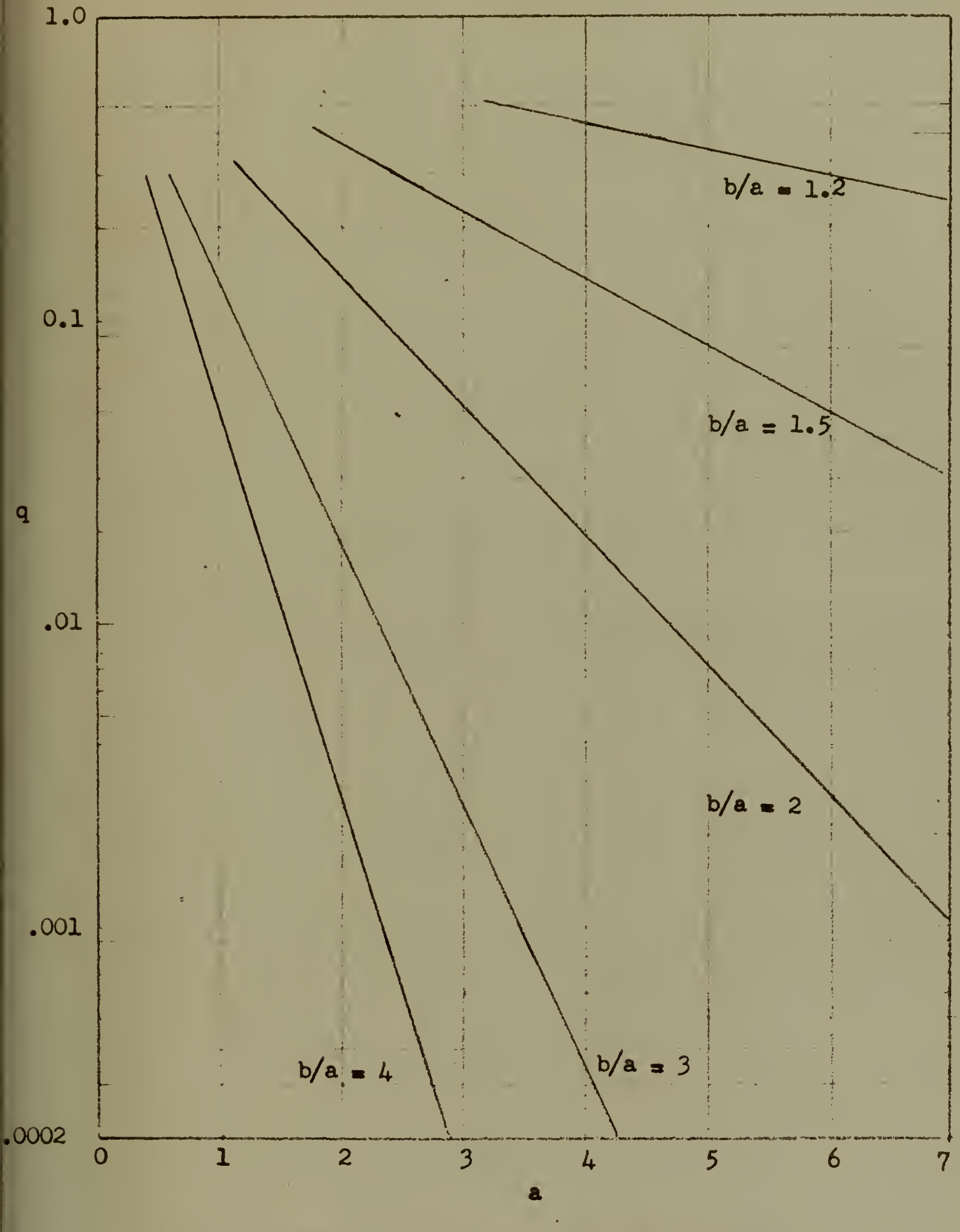

Fig. 24. Coefficient of coupling as a function of helix radii and frequency

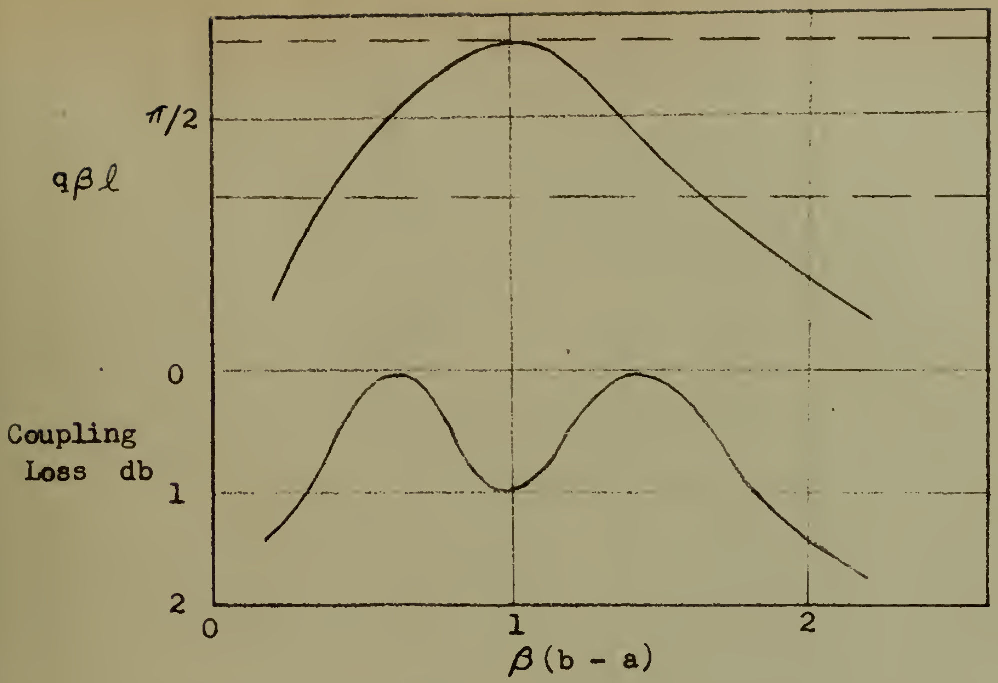

Fig. 25. Variation of qβℓ and coupling loss with frequency and helix radii

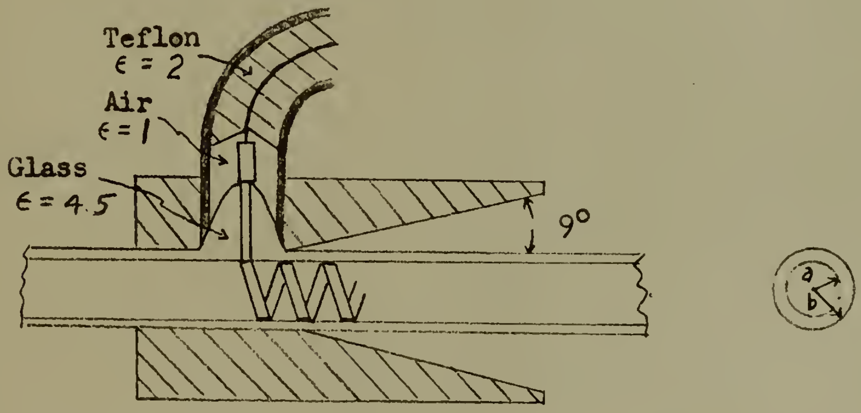

Fig. 26. Tapered shield transition

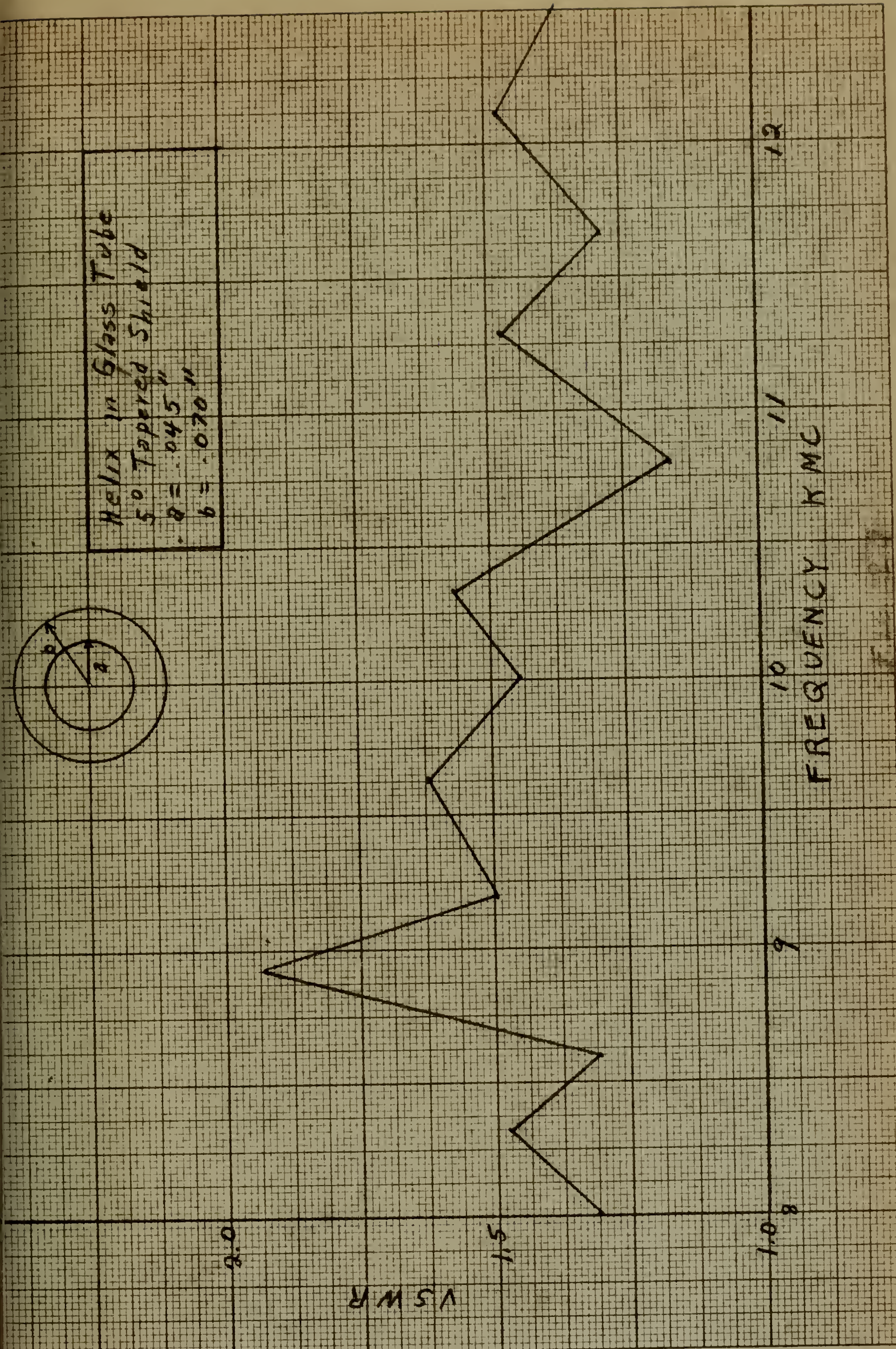
Helix in Glass Tube
5° Tapered Shield
a = .045"
b = .070"
a
b
VSWR
2.0
1.5
1.0
8
9
10
11
12
FREQUENCY KMC

Fig. 27

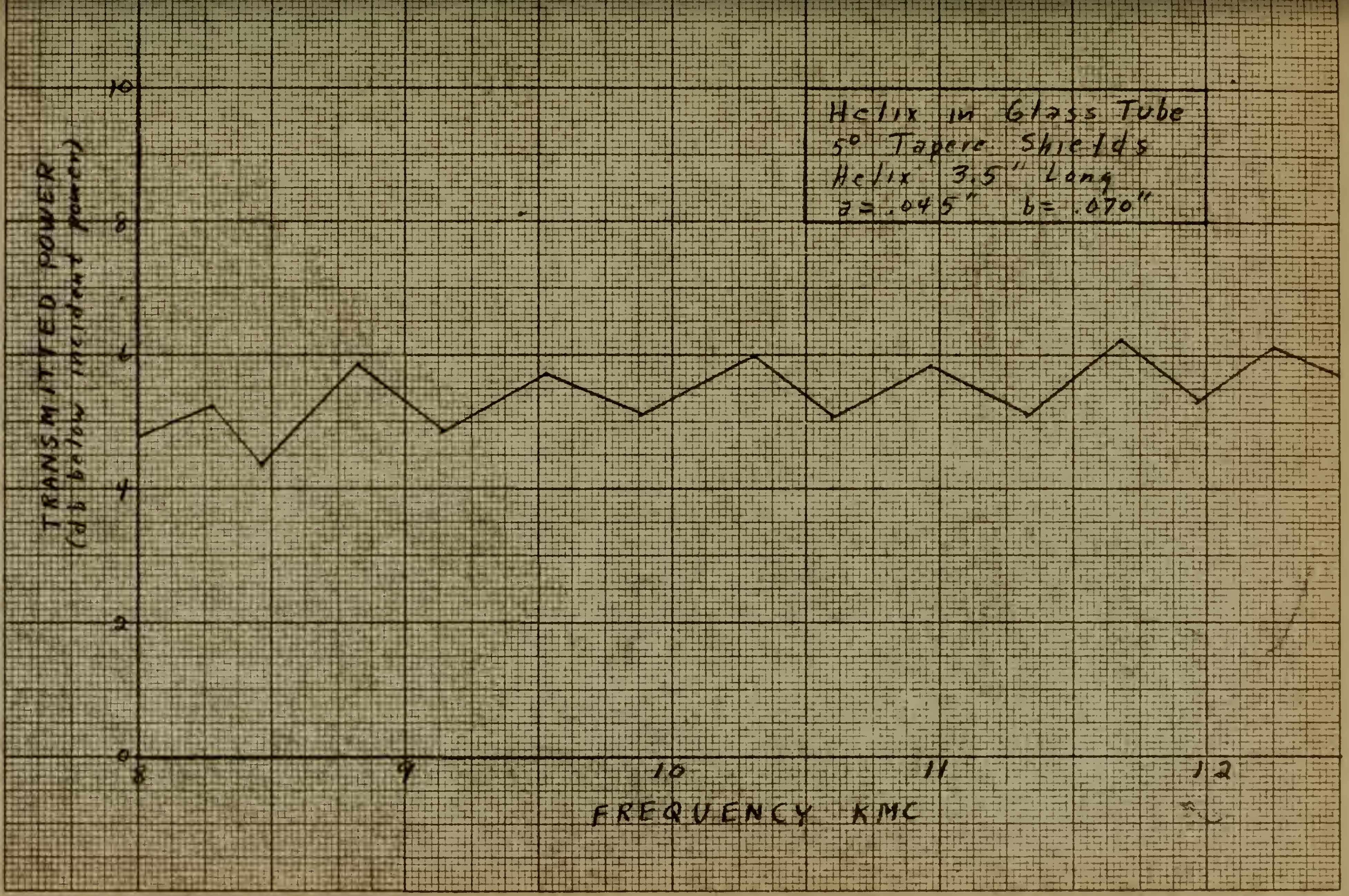
Helix in Glass Tube
5° Tapere Shields
Helix 3.5" Long
a = .045" b = .070"
TRANSMITTED POWER
(db below incident power)
10
8
6
4
2
0
8
9
10
11
12
FREQUENCY KMC

Fig. 28

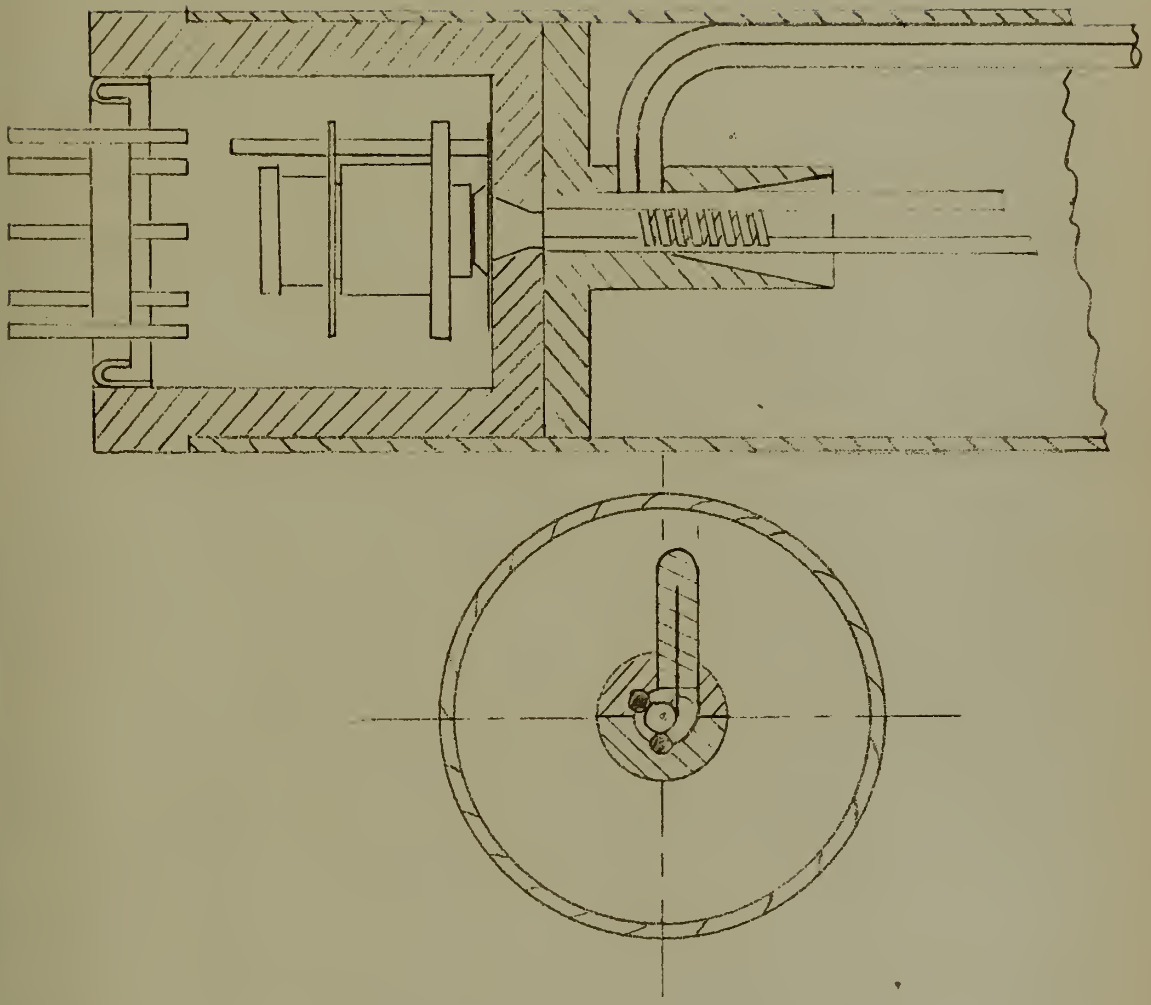

Fig. 29. Tapered shield transition for ruggedized tube

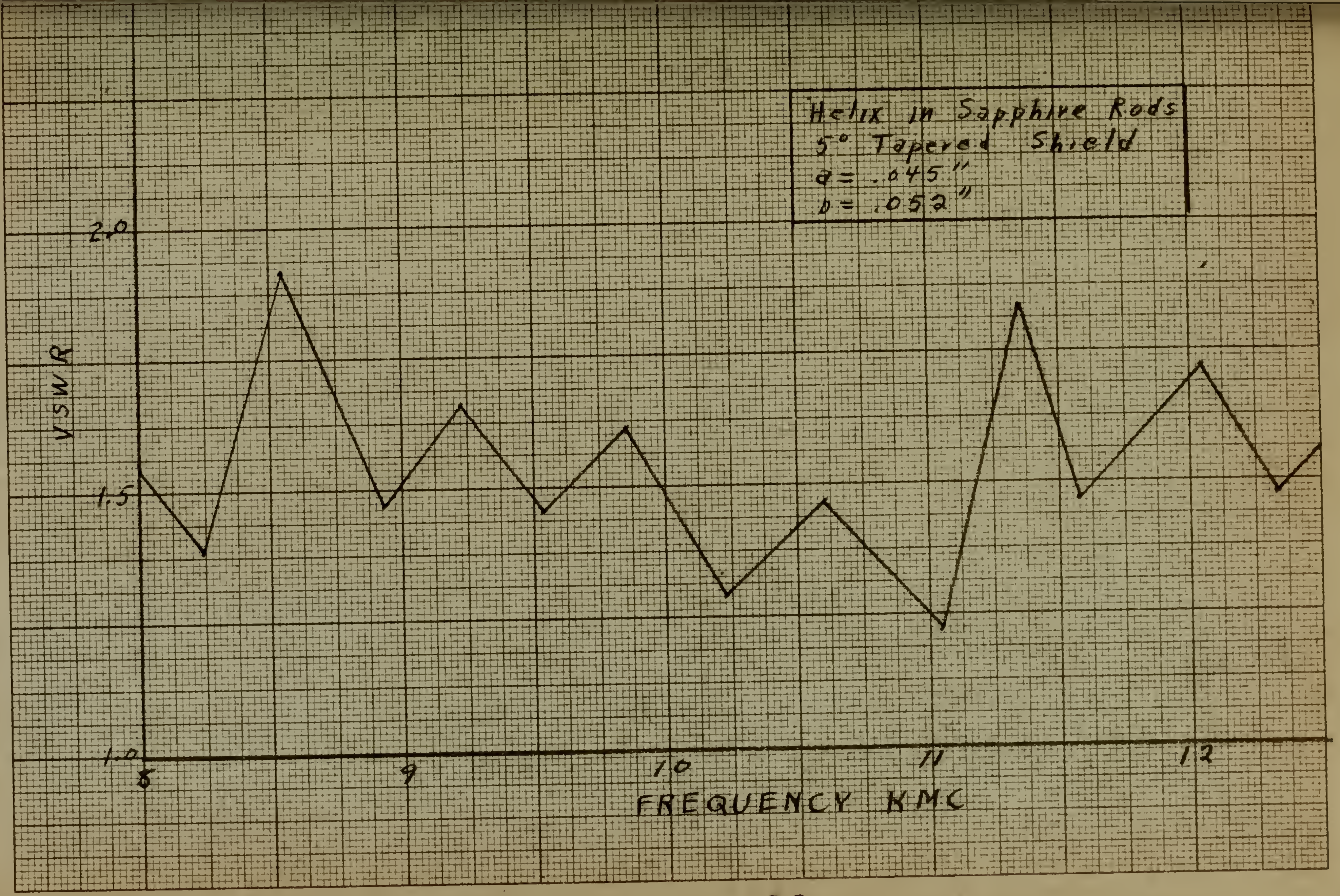
Helix in Sapphire Rods
5° Tapered Shield
a = .045"
b = .052"
2.0
1.5
1.0
VSWR
8
9
10
11
12
FREQUENCY KMC

Fig. 30

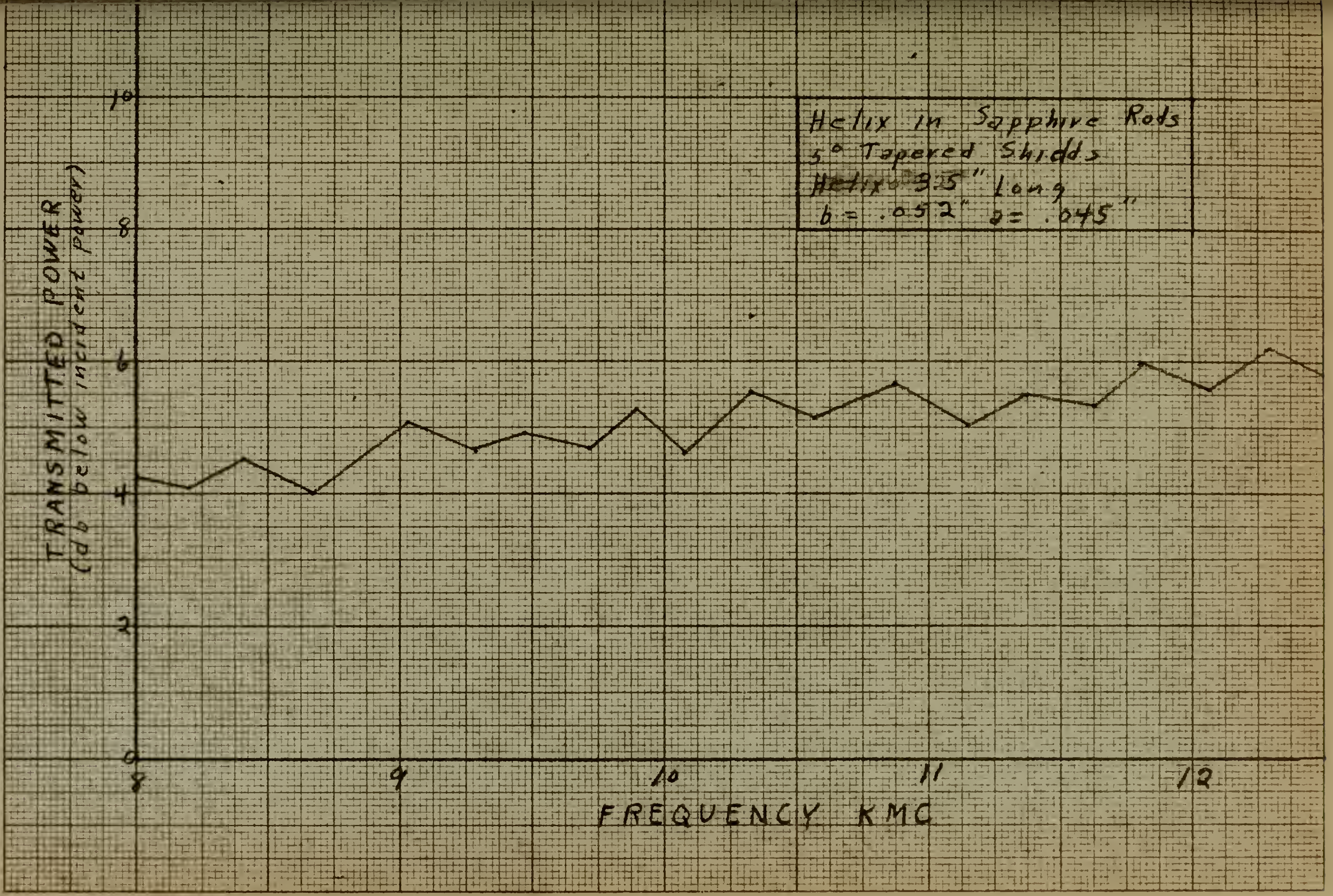
Helix in Sapphire Rods
5° Tapered Shields
~~Helix~~ 3.5" Long
b = .052" a = .045"
TRANSMITTED POWER
(db below incident power)
10
8
6
4
2
0
8
9
10
11
12
FREQUENCY KMC

Fig. 31

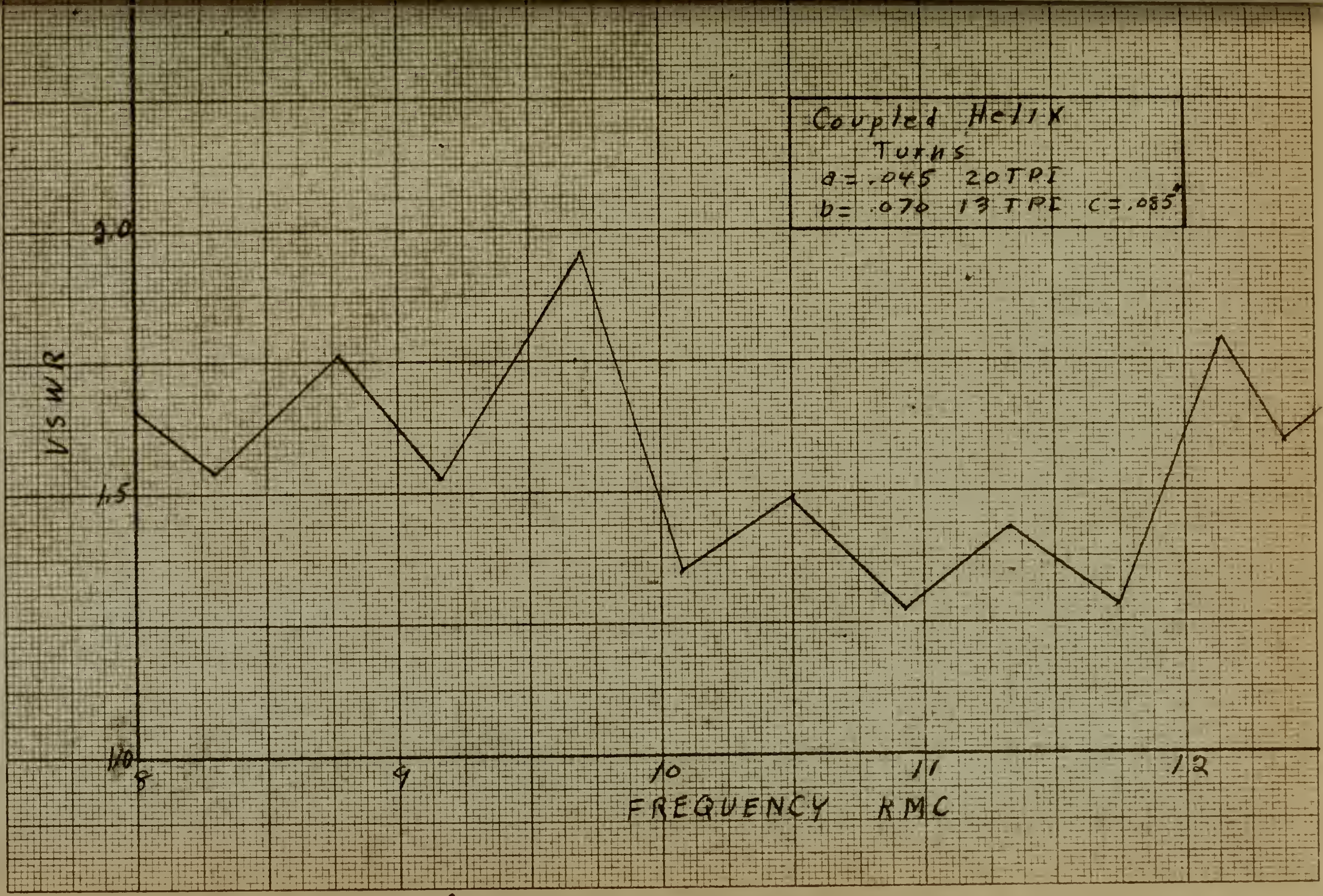
Coupled Helix
Turns
a = .045 20 TPI
b = .070 13 TPI C = .085"
VSWR
2.0
1.5
1.0
8
9
10
11
12
FREQUENCY KMC

Fig. 32

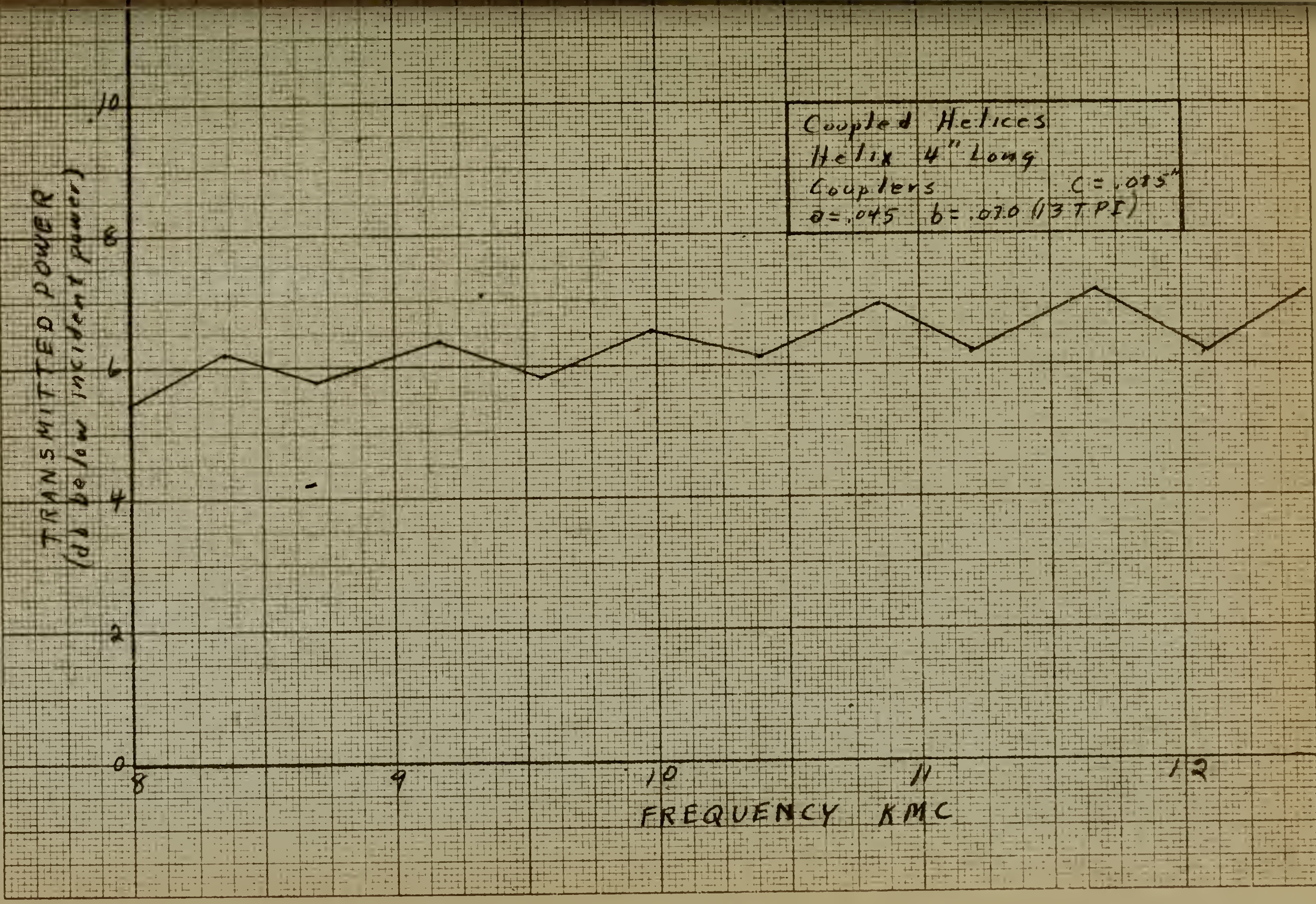
Coupled Helices
Helix 4" Long
Couplers C = .015"
a = .045 b = .070 (13 TPI)
TRANSMITTED POWER
(db below incident power)
10
8
6
4
2
0
8
9
10
11
12
FREQUENCY KMC

Fig. 33

28495
Thesis
H45 Henningsen
Coupling transitions for
traveling wave tubes.

Thesis 28495
H45 Henningsen
Coupling transitions for traveling wave tubes.

thesH45
Coupling transitions for travelling wave
3 2768 001 91859 2
DUDLEY KNOX LIBRARY